KWR | February 2014

Interactions between SOM accumulation, nutrient availability, and plant diversity in lime-rich and lime-poor dune grassland succession

KWR
Watercycle
Research
Institute

Rapport

Interactions between SOM accumulation, nutrient availability, and plant diversity in lime-rich and lime-poor dune grassland succession

KWR | February 2014

Opdrachtnummer
A309519

Projectmanager
E. Dorland

Opdrachtgever
DPW

Kwaliteitsborger
J.P.M. Witte

Auteurs
Y.Fujita, J.W.C. Melis, A.M. Kooijman, C.J.S. Aggenbach

Verzonden aan
DPW-bedrijven

Jaar van publicatie
2014

Meer informatie

T +31 (0)30 60 69 707

E Yuki.Fujita@kwrwater.nl

PO Box 1072

3430 BB Nieuwegein

The Netherlands

T +31 (0)30 60 69 511

F +31 (0)30 60 61 165

E info@kwrwater.nl

I www.kwrwater.nl

KWR Watercycle Research Institute

Managementsamenvatting

Rapport titel
Interactions between SOM accumulation, nutrient availability, and plant diversity in lime-rich and lime-poor dune grassland succession

Auteurs
Y.Fujita (KWR), J.W.C. Melis (UU), A.M. Kooijman (UvA), C.J.S. Aggenbach (KWR)

Datum verschijnen
February 2014

Begeleidingsgroep
H. van der Hagen (Dunea), M. van Til (Waternet), H. Kivit (PWN), D. Groenendijk (PWN)

Rapportnummer
KWR 2014.006

Samenvatting
Effectief beheer en herstel van droge duingraslanden is van groot belang voor duinwaterbedrijven in het kader van nationale maatregelen (Programmatische Aanpak Stikstof) en EU regelgeving (Natura 2000). De biodiversiteit van duingraslanden is in de afgelopen decennia flink afgenomen door vergrassing en struweelvorming, die werden versneld door de hoge stikstofdepositie en daarmee gepaard gaande accumulatie van organische stof. Om beter inzicht te krijgen in het mechanisme van de snelheid van organischestofaccumulatie en diens effecten op de biodiversiteit, onderzochten wij de factoren die invloed hebben op de mineralisatiesnelheid van koolstof en stikstof, en op de productiviteit en biodiversiteit van kalkrijke en kalkarme duingraslanden. Tevens bestudeerden wij de effecten van verschillende bodem-processen en biomassaproductie op de ontwikkeling van duinecosystemen op de lange termijn. Het onderzoek bestond uit veldmetingen en een modelstudie in de Amsterdamse Waterleidingduinen.

Uit het onderzoek blijkt dat de accumulatiesnelheid van koolstof sneller is in kalkrijke duinen dan in kalkarme duinen. Dat komt doordat kalkrijke bodems minder rijk zijn aan micro-organismen die koolstofverbindingen afbreken. Het verschil in stikstofaccumulatiesnelheid tussen kalkrijke en kalkarme duinen was niet groot en de stikstofbeschikbaarheid door mineralisatie was iets hoger in kalkrijke dan in kalkarme bodems. Biomassaproductie was hoger in kalkrijk bodems, want de stikstofbeschikbaarheid is, naast de bodemzuurgraad, een belangrijke factor voor de plantaardige productie. Het aantal plantensoorten was in het algemeen hoger in kalkrijke duinen, maar de factoren die bepalend zijn voor de soortenrijkdom zijn verschillend voor vaatplanten en mossen: een lage bodem-pH is beperkt de soortenrijkdom van vaatplanten, terwijl de soortenrijkdom van mossen minder groot is bij een hoge productie van de kruidlaag. Uit de modelstudie blijkt dat de hoge stikstofdepositie in de jaren 70-90 de accumulatie van organische stof in de bodem heeft bevorderd.

Belang voor DPW
De snelheid van bodemsuccessie wordt beïnvloed door diverse processen, die verschillend uitpakken voor kalkarme en kalkrijke duinbodems en voor verschillende fasen in de successie. De hoge stikstofdepositie in de laatste decennia heeft de accumulatie van organische stof versneld en dat heeft nog steeds invloed op de huidige verhoogde

beschikbaarheid van stikstof. De hoge bovengrondse biomassa van de kruidlaag, veroorzaakt door de hoge stikstofbeschikbaarheid in de late successiefasen, lijkt in kalkrijke duinen nadelig te zijn voor de rijkdom aan korstmossen en mossen. In kalkarme duinen lijkt een lage bodem pH de oorzaak van de lage soortenrijkdom van kruiden. Dus, om de rijkdom aan plantensoorten in duingraslanden te behouden en te bevorderen, zijn verschillende herstel- en beheer maatregelen nodig. Het is daarbij van belang om met uit eenlopende maatregelen herstel op zowel een korte als lange termijn na te streven.

Van belang voor

- Medewerkers van duinwaterbedrijven die beheer- en herstelmaatregelen plannen en evalueren
- Medewerkers van duinwaterbedrijven die belast zijn met de implementatie van PAS en Natura 2000
- Beleidmakers op het gebied van natuurbeheer en implementatie van Natura 2000 en PAS

Trefwoorden

Grijze duinen, ecologisch herstel, organisch stof, stikstofdepositie, bodemsuccessie, vegetatie, biodiversiteit.

Summary

Effective management and conservation of grasslands of Grey dune ecosystems are of great importance for drinking water companies, since they are designated as target ecosystems by national (Programmatische Aanpak Stikstof) and European (Nature 2000) laws. Biodiversity of Grey dunes has severely declined in the last decades due to increased grass and shrub encroachment, which was accelerated by high atmospheric N deposition and concommitant accumulation of soil organic matter (SOM). However, it is still poorly understood how SOM accumulation influences plant production and biodiversity under different conditions of climate, atmospheric N deposition, and soil (e.g. lime-rich and lime-poor soils).

To improve our understandings on the mechanisms of biodiversity decline in Grey dune ecosystems, this study examined in lime-rich and lime-poor dry dune grassland ecosystems: 1) which factors influence turnover rates of soil carbon (C) and nitrogen (N), 2) which factors influence productivity and diversity of plant communities, and 3) how different processes of SOM turnover and plant growth influence the long-term development of soil and plant in dune succession. We combined field measurements in Amsterdamse Waterleidingduinen (AWD) (for the research aim 1 and 2) and modeling study of dune soil development (for the research aim 3). We selected 40 plots in AWD, including both lime-rich and lime-poor sites from four different successional stages, which were established in 2012 by the previous DPW project [*Aggenbach et al*., 2013]. The empirical study included measurements of soil and plant variables, as well as lab incubation experiments of the soils to determine process rates of SOM decomposition. For the modelling study, we modified the internationally-used SOM-hydrology-plant model, CENTURY, to include several important processes in Dutch Grey dune ecosystems. With this modified model, we simulated dune succession, starting from bare sand, using the historical data of atmospheric N deposition and climate. The model output was validated with the observed data in AWD.

Factors differentiating the SOM accumulation rates between lime-poor and lime-rich dunes (research aim 1)
C accumulation was faster in lime-rich sites than in lime-poor sites of AWD. This was most probably due to a faster turnover rate of C in lime-poor sites, caused by a relatively larger microbial biomass in these soils. Besides microbial biomass, C turnover rate was also influenced by soil N: C ratio (i.e. suppressed at low N:C ratio) and soil pH (i.e. suppressed at low pH).
N accumulation speed was not different between lime-rich and lime-poor sites. In addition to the factors which regulate C turnover rates, a number of other factors (stoichiometry of soil substrate and microbes, microbial physical characteristics) seemed to play a role in determining the N turnover rate. More detailed studies are needed to further clarify the mechanisms in lime-rich and lime-poor sites.

Factors differentiating plant biomass and species richness between lime-poor and lime-rich dunes (research aim 2)
Although the turnover rates of N were slower in lime-rich sites, a larger amount of soil total N led to higher N release in these soils.Since the majority of plant communities in this study were N limited, higher amount of nitrogen availability in lime-rich sites led to higher plant biomass in these sites. This higher biomass, however, did not lead to lower plant species diversity: total plant species number was higher in lime-rich sites. When looking at different species groups separately, the number of phanerogams was higher in lime-rich sites whereas moss and lichen species were more abundant in lime-poor sites. It is likely that the former

was caused by negative effect of low pH on phanerogams, whereas the latter was caused by higher sensitivity of mosses and lichens to the shading effects of plant biomass.

Long-term development of dune soils and vegetation, studied by a process-based model of soil, water, and vegetation (Research aim 3)
With the modified version of CENTURY model, C accumulation of long-term (ca. 75 years) dune succession was predicted reasonably well. The accumulation was strongly influenced by the historical atmospheric N deposition: the accumulation speed was particularly fast in 1970's to 1990's when N deposition level was high. N accumulation and plant biomass was poorly predicted by the model, and the observed differences in lime-poor and lime-rich soils could not be properly reproduced by the model. To improve the model prediction, it is needed to use better repro-functions to estimate model input values (e.g. bulk density, soil physical parameters for pF curves) by using data from dune ecosystems. Also, more process-based formulations are needed for a number of key processes in dune ecosystems, such as pH effects on plant growth and soil microbial activity, moisture effects on plant growth, and vegetation-specific evapotranspiration.

To synthesize, this study improved our understanding on the mechanisms of why SOM accumulation speed was different between lime-rich and lime-poor sites in dune succession, which was already observed in the former DPW project [*Aggenbach et al.*, 2013]. The accumulation speed of soil C and N was determined by interplay between microbial abundance, soil N richness, and soil pH, in a specific manner for each successional age. With a process-based model, we could simulate long-term development of dune soils and plants. In order to make the simulation results more realistic, further studies are needed to better parameterize and validate the model for the specific dune ecosystems.

Implication for management
This study provided several implications for restoration of dune ecosystems in AWD and other comparable dune areas in the Netherlands. First, accumulation rate of SOM, an important factor to determine the succession speed of dune ecosystems, was regulated by complicated processes which were different among successional stages and between lime-rich and lime-poor sites. Second, high atmospheric N deposition in the past still has effects on current SOM accumulation and nutrient availability in soils. Removal of top soils or soil renewal would help reducing N availability for phanerogam species. However, accumulation of SOM is a perquisite for species rich dune grasslands and therefore these measures are only effective after 2-3 decades. Other measures which do not remove all SOM, may restore grey dunes faster, but also may be less effective. Third, different mechanisms play roles in determining biodiversity of different plant groups: soil pH seems to be an important determinant for species richness of phanerogams, whereas shading effects of plant biomass seem to strongly influence the number of moss and lichen species. Therefore, in order to conserve plant biodiversity of grey dunes, management plans should include measures which operate on a short (< 20 y) and longer time scale (>20 y) and which improve base status and light conditions.

Table of content

1 Introduction

1.1 Problem definition

Dry dunes host diverse habitat types, including species-rich dune grasslands. Effective restoration and management of these ecosystems are of great concern for dune water companies, as they are designated as target habitats both by national nature policy and European laws (Natura 2000, in which 'grey dunes' (H2130) is a priority habitat type). Elevated atmospheric nitrogen (N) deposition in the last century caused decline in plant biodiversity in these ecosystems due to increased grass and shrub encroachment [*Kooijman et al.*, 1998; *Veer and Kooijman*, 1997]. Although N deposition rates slightly decreased in the last decades, it is still exceeding the critical level [*Bobbink et al.*, 2010]. Also, the accumulated organic matter (SOM) in soil remains and may cause high mineralization rates. Therefore the ecosystems are still under thread for biodiversity loss [*Kooijman et al.*, 2012]. In addition, the expected climate change in near future will affect the grey dunes and may hamper the restoration measures in these ecosystems.

Dry dunes are dynamic systems, consisting of different successional stages such as bare soil, moss-, lichen-, grass-, and shrub-dominated vegetation types. Understanding the mechanisms and drivers of succession processes is thus the key to properly predict the effects of restoration measures, atmospheric N deposition, and climate change. In general, SOM accumulates and plant biomass increases along with succession, and a chain of feedback processes occurs accordingly. For example, the accumulated SOM leads to higher availability of nutrient (e.g. nitrogen (N) and phosphorus (P)) for plants, not only because it contains higher amount of nutrients, but also because higher SOM contents improves water retention in soil and therefore facilitate microbial activity to break down SOM. The change in nutrient availability will affect growth of plants, which will eventually influence evapotranspiration and nutrient input to soil via plant litter and roots. Moreover, the changes in species composition of plant community and microbial community in soil may influence the magnitudes or directions of the above-mentioned feedback mechanisms.

Empirical studies showed that the accumulation speed of SOM was influenced by multiple factors. It is accelerated by high atmospheric N deposition and temperature [*Jones et al.*, 2008], and was faster in lime-rich than lime-poor sites [*Aggenbach et al.*, 2013]. Availability of N and P are known to be different between lime-poor and lime-rich dunes too [*Kooijman et al.*, 1998], possibly due to difference in microbial demands for nutrients [*Kooijman and Besse*, 2002] or due to effects of soil pH on decomposition processes [*Walse et al.*, 1998]. These differences may have a link to the contrasting patterns of plant species diversity in lime-poor and lime-rich dunes [*Aggenbach et al.*, 2013; *Kooijman et al.*, 1998]. However, the exact mechanisms how SOM accumulation and nutrient cycling are regulated in lime-rich and lime-poor sites are still poorly understood.

Process-based models will help to disentangle the interacting processes of SOM, water, and plants in dune succession. The models will enable to quantify magnitude of influence of multiple factors on SOM accumulation and nutrient availability. Furthermore, such models can be used to predict future development of dune ecosystems under different scenarios of climate and nature management.

1.2 Research aims

In order to improve our understanding on the processes and drivers of dune succession in lime-rich and lime-poor areas, we focus on three aspects. Firstly, we aim at clarifying the difference in SOM accumulation speed and nutrient availability in lime-rich and lime-poor

areas in the course of succession. Secondly, we examine the factors which determine the plant diversity patterns in lime-rich and lime-poor areas. Thirdly, we explore how different processes of SOM turnover and plant growth influence the long-term development of soil and plant in dune ecosystems.

Our research aims are:

1. To examine factors differentiating the SOM accumulation rates between lime-poor and lime-rich dunes
2. To examine factors differentiating plant biomass and species richness between lime-poor and lime-rich dunes
3. To understand the long-term development of dune soils and vegetation, by developing a process-based model of soil, water, and vegetation and by validating the model for lime-poor and lime-rich dunes

1.3 Approach

We combined empirical measurements in Amsterdamse Waterleidingduinen (AWD) (for the research aim 1 and 2) and modeling study of dune succession using the modified version of the model CENTURY (for the research aim 3). We selected both lime-rich and lime-poor plots from four different successional stages, which were established in 2012 by the previous DPW project [*Aggenbach et al.*, 2013]. The empirical study included measurements of soil and plant variables, as well as lab incubation experiments of the soils to determine process rates of SOM decomposition. For the modeling study, we used the internationally-used SOM-water-plant model CENTURY [*Parton et al.*, 1987]. We modified the model to include several important processes in Dutch grey dune ecosystems. In addition, we simulated dune succession from bare sand, using the historical data of atmospheric N deposition and climate. The model outputs were validated with the measurement data on SOM accumulation and plant productivity from different successional stages in AWD.

2 Materials and Methods

2.1 Site selection

Our plots consist of lime-rich and lime-poor areas with different succession stages in Amsterdamse Waterleidingduinen (AWD). We used a part of the plots established by *Aggenbach et al.* [2013] for the DPW-onderzoek A309202. The succession age of each plot was estimated by analysing the historical aerial photographs [see *Aggenbach et al.*, 2013 for details of the age estimation]. We selected five succession age classes (0, 6-11, 33-44, 54-74, and >74 years) in lime-rich and lime-poor areas, for which 5 replicas were taken. In total 50 plots were sampled in April 2013 (Figure 1, Tabel 1). Because the distinction between lime-poor and lime-rich classes turned out to be obscure for the age class 54-74 years, we excluded these plots (N=10) from the analysis.

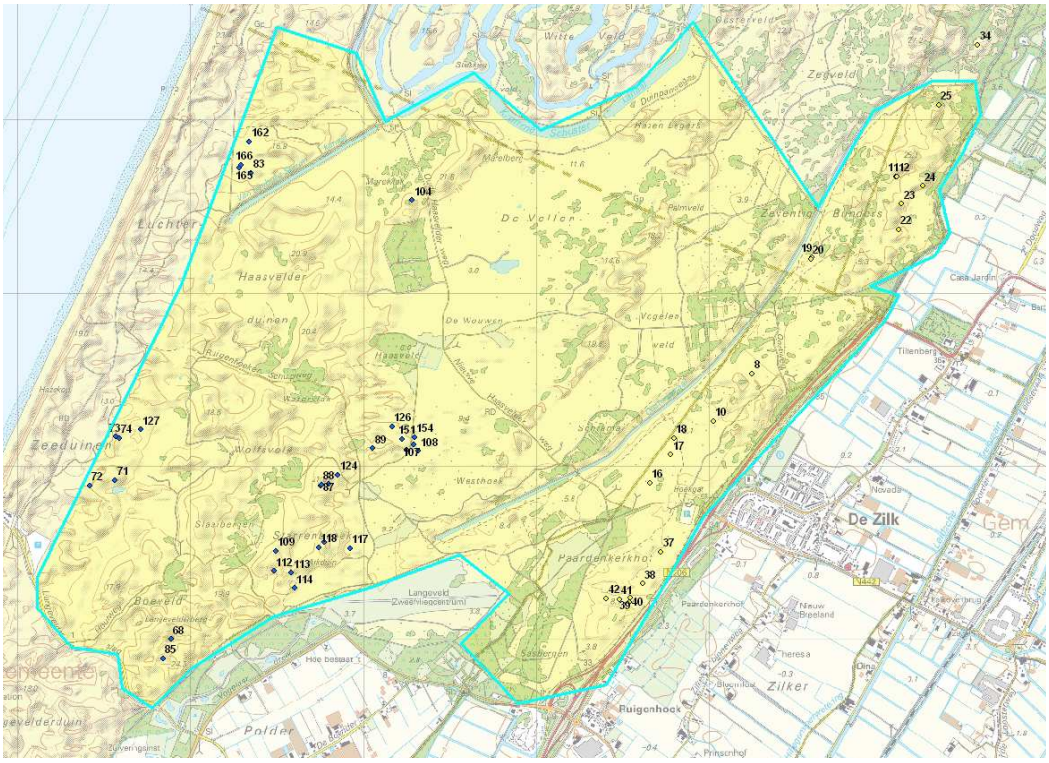

Figure 1. The 50 selected plots in AWD. Yellow and blue points indicate lime-poor and lime-rich plots, respectively.

Tabel 1. Overview of selected 50 plots in AWD. The age class 54-74 years did not have clear distinctions in the lime class and therefore not used in the statistical analyses.

Age (year)	Lime class	Plot number
0	Lime-poor	16, 17, 18, 19, 34
	Lime-rich	85, 123, 124, 126, 127
6-11	Lime-poor	20, 22, 23, 24, 25
	Lime-rich	68, 83, 87, 88, 89
33-44	Lime-poor	8, 10, 11, 12, 42
	Lime-rich	71, 72, 73, 74, 105
54-74	-	104, 107, 108, 109, 110
	-	112, 113, 114, 117, 118
>74	Lime-poor	37, 38, 39, 40, 41
	Lime-rich	151, 154, 162, 165, 166

2.2 Soil bulk measurements

Soil samples were collected in the field between 2nd and 5th April 2013. There was no rainfall during the sampling period. We sampled the mineral soils (i.e. not including litter) in the depth of 0-5 cm using a metal core. In order to minimize the effect of small-scale heterogeneity of the soil, five soil cores were sampled in each plot to make a composite soil sample. Each composite sample was mixed in a polyethylene bag, and stored in the fridge at 4 ˚C until further analysis.

Soil dry weight (g d.w. soil) was determined by drying the soils for 24 hours at 105 ˚C. Gravimetric soil moisture content (w_g, g water g d.w. soil^{-1}) was calculated as the fraction of water per dry soil. Note that w_g was measured at a specific moment of the year and therefore only partly reflect the moisture regime of the site. Soil bulk density (*BD*, g d.w. soil cm^{-3}) was estimated by the weight and volume of the composite soil samples. Soil pH (pH-H_20) was determined in KWR after extracting 10 gram of fresh soil with 25ml demineralized water, shaken for two hours, and centrifuged at 2000 rpm. Before and between measurements the pH meter was calibrated with standard solutions of pH 4, 7 and 10. With dried and ground soil samples, soil total C (%) and soil total N (%) were determined using CNS analyser (Laboratorium van het Instituut voor Biodiversiteit en Ecosysteem Dynamica, UvA). Note that the soil total C includes C incorporated in $CaCO_3$. See appendix I for the estimates of the C in $CaCO_3$ in each site.

Soil density (ρ_s, g cm^{-3}) was estimated using the formula of *Heinen* [2006]:

$$\rho_s = \left(\frac{SOM}{147} + \frac{Clay}{275} + \frac{Silt + Sand}{266} \right)^{-1}$$

where *SOM* is soil organic matter (%), *Clay*, *Silt*, and *Sand* are their content (%) in the mineral soil. We approximated SOM as twice as soil total C, and assumed 0% clay, 0% silt, and 100% sand contents. Subsequently, pore space of the soil (φ_p, cm^3 cm^{-3}) was estimated as follows [*Heinen*, 2006]:

$$\varphi_P = 1 - \frac{BD}{\rho_s}$$

Volumetric water content in the soil (θ, cm^3 cm^{-3}) was computed as:

$$\theta = w_g \cdot \frac{BD}{\rho_l}$$

where ρ_l is the density of water (g cm^{-3}). ρ_l was set to be 1g cm^{-3}.
Finally, water filled pore space (*WFPS*, fraction) was computed as:

$$WFPS = \frac{\theta}{\varphi_P}$$

For three replicas of soil samples per category, microbial biomass in soils was estimated by substrate induced respiration (SIR) method [*Anderson and Domsch*, 1978]. After 11 weeks stored in the fridge at 4 ˚C, ca. 2g of fresh soil samples were filled in glass jars of ca. 85 ml and the bulk density was adjusted to mimic the field condition by carefully pressing the soils. Ca. 24 hours prior to analyses, soil samples were brought up to room temperature and soil moisture was adjusted by adding demineralized water (so that the WFPS became 80% after the following addition of glucose solution). One hour before analyses 1ml of a glucose 0.1 M solution was added to each soil. CO_2 accumulation in the head space was measured with gas-chromatograph (see the section "soil incubation experiment" for more details). Microbial biomass (*MicC,* mg C/kg soil) was estimated based on the empirical relationship of *Anderson and Domsch* [1978]:

$$MicC = 40.4 \cdot CO_2 + 0.37$$

where CO_2 is the accumulation speed of CO_2 (µl CO_2/g soil/h).
Subsequently, the microbial fraction (*MicC/C,* gC/kgC) was calculated by dividing microbial C

by soil total C.
The CO_2 accumulation was negative for one soil sample (plot 16, age 0 year). This plot was excluded from all analysis concerning microbial C.

2.3 Soil incubation experiments

We conducted soil incubation experiments for 8 weeks to estimate C and N mineralization rates. Ca. 140 g of fresh soil samples were put in glass jars of ca. 85 ml. The soil bulk density was adjusted to mimic the field conditions by carefully pressing the soils. Soil moisture was adjusted to ca. 50% water filled pore space by adding demineralized water. The jars were placed in a dark climate chamber at a temperature of 22 ˚C and humidity of ca. 50%. A small opening on the top of the jars was kept open to allow exchange of air.

Carbon mineralisation was measured twice, at the 5th and 55th day of the incubation period. For each time, CO_2 concentration was measured with a gas-chromatograph (TraceGC Ultra, Interscience) in KWR for three times with intervals of ca. 30-60 minutes by extracting 100 ul of the headspace air of the incubation jar. Reference gas of known CO_2 concentrations (ca. 0.4%, 0.8% and 1.6% in volume) was made by mixing 100% CO_2 and 100% N_2. Using the reference gas, the CO_2 concentrations of the extracted air was converted to mg C/L with the assumption of CO_2 density of 24.5 (mol/L). Subsequently, for each soil sample, increase in CO_2 concentrations per soil per hour (mgC/g dry soil/h) was estimated from the slope of linear regression model of the three measurements. Finally, the cumulative CO_2 release from the soils during the the entire incubation period (*Cmin*, gC/g d.w. soil/56 days) was calculated based on the slopes of the 5th day and the 55th day (see Appendix II). In addition, to correct for the SOM size among different soils, C mineralization rates per soil total C (*Cmin/C*, gC/gC/56 days) were computed. *Cmin/C* can also be interpreted as the rate of C turnover.

N mineralisation was estimated as the increase in extractable N during the incubation period. At the beginning and the end of the incubation, ca. 50 gram of fresh soil was mixed with 100 ml 0.001M CaCl2 solution, shaken for 2 hour, centrifuged at 2000 rpm, and filtered through 1.2 µm syringe filters (Whatman GF/C). The extracts were analysed for NH_3 and NO_2/ NO_3 with a flow analyser (SFA-$CaCl_2$) at the 'chemisch biologisch laboratorium bodem' in WUR. Due to practical constrains, the dates of the second measurement were not identical for all soil samples (i.e. 56th day for 22 samples, 57th day for 11 samples, 58th day for 3 samples and 59th day for 14 samples). For simplicity, we considered that all soil samples were measured at the 56th day after the start of the incubation. The extractable N concentration of a soil sample (i.e. plot 165; lime rich, age >74) was unrealistically high, probably due to contamination. We excluded this sample for all the analysis concerning N mineralization.
N mineralization rate (*Nmin*, gN/g d.w. soil/56 days) was calculated from the increase in N-NH_4 + N-NO_2/NO_3 concentrations between the two measurements. To correct for SOM size difference among soils, N mineralization rates per soil total C (*Nmin/C*, gN/gC/56 days) and N mineralization rates per soil total N (*Nmin/N,* gN/gN/56 days; this can be interpreted as N turnover rate) were also computed.

2.4 Plant measurements

For each plot, plant species (phanerograms, bryophytes, and lichens) were identified in 1x1m in 2012 [*Aggenbach et al.*, 2013]. Above-ground plant biomass of 0.25x0.25m was harvested in 2012, and weighed after drying at 60 ˚C [*Aggenbach et al.*, 2013]. The biomass sample of a plot (plot 83, age 6-11 years) was missing. We excluded this plot from all the analysis concerning plant biomass and nutrient contents.

From the dried vegetation sampled in 2012, we determined nutrient contents in plants. The plots in the age category 0 year were excluded because they contained almost no biomass. C and N content was determined from ca. 8 mg of ground plant biomass with CNS analyser in

UvA. P and K content was determined by acid destruction with HNO_3/HCl mixture [*Bettinelli et al.*, 1989]. 250 mg of ground plant biomass were mixed with 4 ml of HNO_3 (65%) and 2 ml of HCl (37%), left to react for 60 min, then 1 ml demineralised water was added. Samples were put in a microwave (30 min at ca. 200 ˚C, 75 bars). Destructed samples were analysed for phosphorus and potassium in an ICP analyser in UvA.

The type of nutrient limitation for plant growth can be detected from the ratio of elements in above-ground plant biomass [*Olde Venterink et al.*, 2003]. For that reason we calculated N:P ratio, N:K ratio, and K:P ratio in plant biomass, and checked which element (N, P or K) is limiting in each plot. We used the threshold values of *Olde Venterink et al.* [2003]: a plot was considered as N-limited if N:P<14.5 and N:K<2.1; P- or P+N-limited if N:P>14.5 and K:P>3.4; and K- or K+N-limited if N:K>2.1 and K:P<3.4.

2.5 Statistics

The list of all soil and plant variables tested is shown in Tabel 2. Prior to the analyses, a number of soil variables and plant variables were transformed to correct for right-skewed distribution (i.e. log-transformation for *soilC*, *soilN*, w_g, *MicC/C*, *Cmin*, *Cmin/C*, *Nmin/N, plantNK*, *Biomass*; square-root-transformation for *Nmin* and *Nmin/C*).

To examine the effect of age class (0/6-11/33-44/>74 years), lime class (lime-rich/lime-poor), and their interactions on soil and plant variables, 2-way ANOVA was conducted. The equality of the variance was tested with Levene test, and the normality of the residual values were tested with Shapiro-Wilk test at the significance level of p=0.05. The difference among the categories was tested with multiple comparison test (Turkey HSD).

To explore the factors influencing *Cmin/C*, a series of regression analyses was conducted. First, bivariate linear regression analyses were conducted for *Cmin/C* with *pH*, *MicC/C*, and *soilNC*. Both 1st and 2nd order of the explanatory variables were tested, and we included only those for which the coefficients were significantly ($p<0.05$) different from zero. Subsequently, we conducted a multivariate regression analysis with the three explanatory variables (including the 2nd order, if it was included in the bivariate regression analysis). The best model was selected with stepwise selection, using AIC.
The same series of regression analyses were conducted for *Nmin/C* with *pH*, *MicC/C*, and *soilNC*; for *biomass* with *pH*, *Nmin*, and *moisture*; for *sp_pha* with *pH* and *biomass*; and for *sp_bry* with *pH* and *biomass*. For all regression analysis, we tested if the residual values were normally distributed (Shapiro-Wilk test).

All analysis was conducted using the programming language R [*R Development Core Team*, 2013].

2.6 Simulation of dune succession

2.6.1. Model adjustment

Succession of dune soil and vegetation was simulated using an internationally-used CENTURY model [*Parton et al.*, 1987; *Parton et al.*, 1993]. We reconstructed the CENTURY model using the programming language Python 2.7.3. We used the modified version of the decomposition module which has been validated for various Dutch soil conditions [*Fujita et al.*, 2013]. For the rest of the model, equations of CENTURY version 4 [*Metherell et al.*, 1993] were used unless specified. See Appendix III for the structure and equations of our model.

To make the CENTURY model more applicable for the simulation of dune succession, we made several modifications in the CENTURY model. That are: i) effects of slope and exposition on evapotranspiration, ii) feedback effects of SOM accumulation on soil physical characteristics, and iii) changes in soil pH along succession and its effects on SOM decomposition.

(i) The effect of slope angle (*sag*, degrees) and aspect (*sas*, degrees; e.g. East is 90˚, South is 180˚) on potential transpiration rate (*Tp*, cm/day) was formulated based on an empirical relationship [*Jansen and Runhaar*, 2005]):

$$Tp' = Tp + Tp \cdot f_{\mathrm{SLP}}$$

$$\begin{cases} f_{\mathrm{SLP}} = \dfrac{sag}{100} \cdot \dfrac{sas - 90}{90} & sas < 180^\circ \\ f_{\mathrm{SLP}} = \dfrac{sag}{100} \cdot \dfrac{270 - sas}{90} & sas \geq 180^\circ \end{cases}$$

where f_{SLP} is the slope factor. South slopes are associated with positive f_{SLP} values, whereas North slopes are associated with negative f_{SLP} values. The steeper the slope is, the larger the f_{SLP} value is.

(ii) The influence of SOM increase on soil physical characteristics was incorporated by annually updating the parameter values based on SOM accumulation. Among the pF curve parameters, θ_{sat} of top soils (cm^3/cm^3) is updated annually according to the repro function of *Heinen* [2006]:

$$\theta_{sat} = 1 - BD / \rho_s$$

where *BD* is the bulk density (g/cm^3) and ρ_s is the soil density (g/cm^3). The other pF curve parameters (θ_{res}, α, n) remain unchanged during simulation.

The *BD* was calculated using the repro function of *Wösten et al.* [2001] for sandy soils in upper soils ('bovengrond'):

$$BD = \left(-7.5474 + 0.01791 \cdot SOM - 0.00338 \cdot M50 + 157.7/M50 + 1.522 \cdot \ln\left(M50\right) + 0.3937 \cdot Tex^2\right)^{-1}$$

where *SOM* is the organic matter content (%) of the beginning of the year, *M50* is the median diameter of the sand fraction (micrometer), and *Tex* is the fraction of sand + silt content in soil.

Subsequently, water content at field capacity (θ_{fc}, cm^3/cm^3) and wilting point (θ_{wp}, cm^3/cm^3) for each soil layer are also annually updated as follows [*van Genuchten*, 1980]:

$$\theta_{fc} = \theta_{\mathrm{res}} + \frac{\theta_{\mathrm{sat}} - \theta_{\mathrm{res}}}{\left[1 + \left(\alpha \cdot 100\right)^n\right]^{\left(1 - \frac{1}{n}\right)}}$$

$$\theta_{wp} = \theta_{\mathrm{res}} + \frac{\theta_{\mathrm{sat}} - \theta_{\mathrm{res}}}{\left[1 + \left(\alpha \cdot 16000\right)^n\right]^{\left(1 - \frac{1}{n}\right)}}$$

(iii) The decrease in pH along succession was approximated for lime-rich and lime-poor sites separately, based on the empirical relationships of *Aggenbach et al.* [2013]:

$$\text{Lime-poor:} \quad pH = 3.80 + 4.77 \cdot \exp\left(-age / 23.6\right)$$

$$\text{Lime-rich:} \quad pH = 5.78 + 2.55 \cdot \exp\left(-age / 21.3\right)$$

where *age* is the year since the start of the simulation from a bare soil.

The effect of soil pH on decomposition of SOM (*Pd*, fraction) was formulated according to *Walse et al.* [1998]:

$$Pd = \frac{1}{1 + K_{pH} \cdot 10^{(-pH)}}$$

where K_{pH} is the coefficient of the reduction term, *pH* is the pH of top soil. We used the K_{pH} value of 20500, the estimate for Holocellulose decomposition [*Walse et al.*, 1998].

2.6.2. Model input values

We started the dune succession from bare sands, containing no C and N in soil and no plant litter. The soil physical characteristics (i.e. soil texture, bulk density, and parameter values of pF curves) were defined based on the 'bouwsteen O1' [*Wösten et al.*, 2001]. The simulation was done for 75 years (from 1938 to 2012), 38 years (from 1975 to 2012), and 8 years (from 2005 to 2012); which correspond to the three major age classes of the measured plots. Climate data of year 1938 to 2012 (i.e. daily minimum and maximum temperature, precipitation, and potential evapotranspiration) were retrieved from De Bilt station of KNMI. The initial water content in the soil was determined by running the hydrological module for 1 year prior to the main simulation routine. A long-term atmospheric N deposition data on a local scale is not available. Therefore we used the national average values of the Netherlands from 1938 to 2004 [*Noordijk*, 2007] (Figure 2). N deposition levels from 2004 to 2012 were assumed to be unchanged.

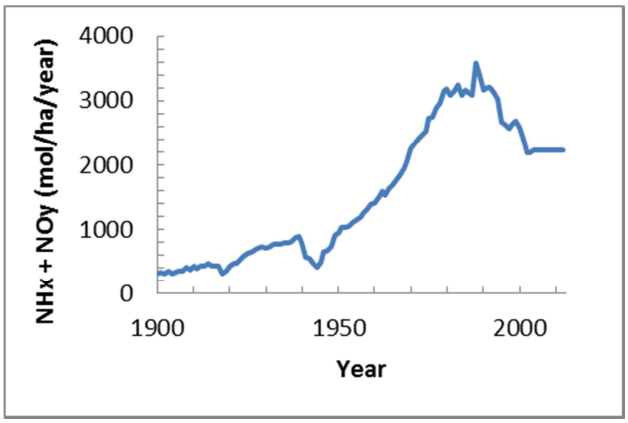

Figure 2. Annual atmospheric N deposition level used in the simulation study.Data source: Noordijk [2007]

2.6.3. Model validation

Simulated soil total C, soil total N, and plant above-ground biomass were compared with the measured average values in AWD in 2012 [*Aggenbach et al.*, 2013]. The selected categories of the AWD plots were those with age category 0, 3-11, 33-44, and >74, for both lime-rich and lime-poor sites.

Additionally, to validate the slope effects included in the model, we compared the slope factor of the site (f_{SLP}) with observed values of soil total C, gravimetric soil moisture, and plant biomass. For each age category, the response variables were regressed by lime class (dummy variable) and f_{SLP}. When the coefficient value of f_{SLP} was significantly ($p<0.05$) different from 0, we considered that slope had a significant effect on the response variable.

Tabel 2. List of soil and plant variables tested. For each variable, results of 2-way ANOVA (F values and their p values) are shown for the effect of lime category (lime-rich/lime-poor), age category (0/6-11/33-44/>74 years), and their interactions. F values with p<0.05 are shown with bold letters.

				ANOVA		
Description	**Unit**	**Abb.**	**N**	**Lime**	**Age**	**Interaction**
Soil total Carbon	%	*soilC*	40	**15.393*****	**60.308*****	0.794
Soil total Nitrogen	%	*soilN*	40	2.569	**119.18*****	0.586
Soil N:C ratio	gN/gC	*soilNC*	40	0.479	**78.409*****	2.705
Soil pH_H2O	-	*pH*	40	**22.33*****	**51.33*****	**4.439***
Gravimetric soil moisture	g water/g soil	w_g	40	3.617	**64.49*****	0.954
Soil bulk density	g soil/cm3	*BD*	40	0.045	**44.448*****	0.803
Microbial Carbon	mgC/kg soil	*MicC*	23	0.488	**15.628*****	0.152
Microbial C per total soil C	gC/kgC	*MicC/C*	23	**13.845****	**6.560****	1.809
C mineralisation rate	gC/kg soil/56d	*Cmin*	40	0.206	**49.962*****	1.355
C mineralisation rate per soil total C (i.e. C turnover rate)	gC/gC/56d	*Cmin/C*	40	2.238	**10.668*****	0.695
C mineralisation per microbial C	gC/gC/56d	*Cmin/micC*	23	**4.980***	**5.139***	**5.806****
N mineralisation rate	mgN/kg soil/56d	*Nmin*	39	**6.389***	**48.427*****	1.297
N mineralisation rate per soil total C	gN/gC/56d	*Nmin/C*	39	0.315	2.468	0.915
N mineralisation rate per soil total N (i.e. N turnover rate)	gN/gN/56d	*Nmin/N*	39	0.224	**12.12*****	0.275

N mineralization rate per C mineralization rate	gN/gC	*Nmin/Cmin*	38	1.515	**5.010****	1.673
Plant N:P ratio	gN/gP	*plantNP*	29	3.263	1.365	1.688
Plant K:P ratio	gP/gK	*plantKP*	29	0.633	0.561	**3.472***
Plant N:K ratio	gN/gK	*plantNK*	29	0.580	0.620	0.368
Plant biomass	g/m2	*Biomass*	39	3.615	**41.185*****	**2.964***
Total species number		*sp_nr*	40	**4.40***	**19.92*****	1.580
Phanerogam species number		*Pha_sp_nr*	40	**24.536****	**15.323*****	2.705
Bryophyte+Lichen species number		*Bry_sp_nr*	40	**10.106****	**10.443*****	**4.117***

****: p<0.001, **: p<0.01, *: p<0.05, without asterisks: not significant.*

3 Results

3.1 Soil development along succession

3.1.1. Soil bulk properties

Soil total C increased with age ($p<0.001$), with a higher rate for lime-rich than lime-poor sites ($p<0.001$) (Figure 3a). Soil total N also increased with age ($p<0.001$), yet the difference between the lime classes was not significant ($p=0.119$) (Figure 3b). Soil N:C ratio increased with age ($p<0.001$) but was not different between the lime classes ($p=0.49$), although it was slightly lower for lime-poor sites in later ages (interaction effect almost ($p=0.062$) significant) (Figure 3c).

Soil pH was lower at lime-poor sites ($p<0.001$) and decreased with age ($p<0.001$) (Figure 3d); the difference between the lime classes becomes larger at later successional age (interaction effect $p<0.01$). Note that the pH values in our study were systematically higher (ca. point 1) compared to those measured in 2012 from the same depth. The difference could have been caused by the use of different pH meters.

Gravimetric soil moisture content increased with age ($p<0.001$, Figure 3e) whereas bulk density decreased with age ($p<0.001$, Figure 3f). The effect of lime class was not significant ($p>0.05$) for both moisture content and bulk density.

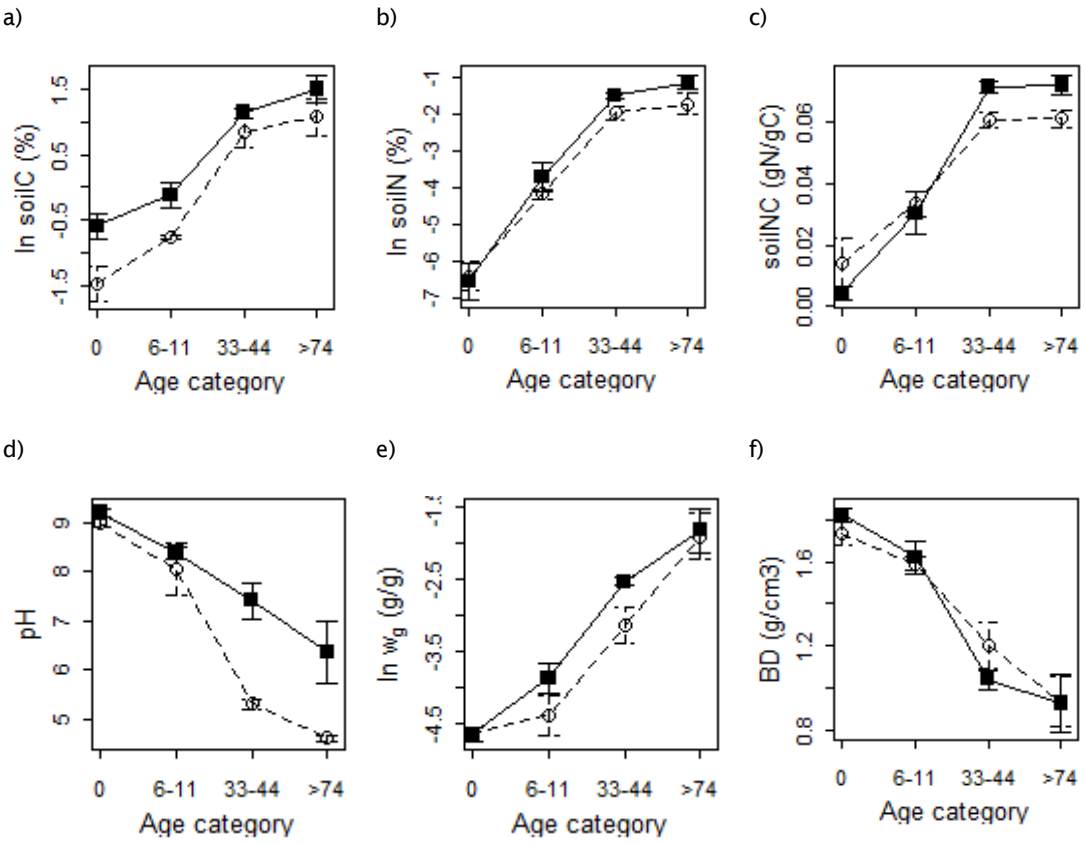

Figure 3. Mean values of a) soil total C, b) soil total N, c) soil N:C ratio, d) soil pH, e) gravimetric soil moisture, f) soil bulk density for each age category of lime-rich (filled squared) and lime-poor (open circles) sites. Bars indicate standard errors.

Microbial C increased with age ($p<0.001$) (Figure 4a). However, when expressed as a fraction of soil total C (i.e. as *MicC/C*), the trend along succession age becomes smaller ($p<0.01$): it slightly decreased in later ages. MicC/C was significantly higher for lime-poor sites ($p<0.01$) (Figure 4b).

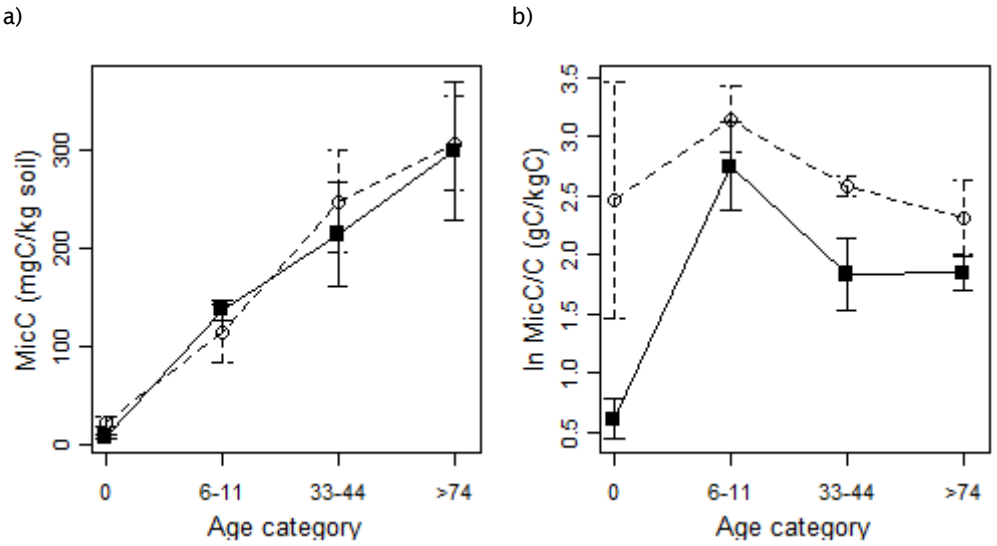

Figure 4. Mean values of a) microbial C and b) microbial fraction for each age category of lime-rich (filled squared) and lime-poor (open circles) sites. Bars indicate standard errors.

3.1.2. C mineralization rates

Soil C mineralization rates during the incubation period increased with age ($p<0.001$) (Figure 5a). When corrected for soil total C (i.e. C mineralization per soil total C (or C turnover rate), *Cmin/C*), the effect of age was also significant ($p<0.001$) but the trend changed: it was significantly lower for the 0-year-old sites (multiple comparison test, $p<0.05$), and in the later stages it decreased with age (although not significantly different among ages). *Cmin/C* was slightly higher in lime-poor sites except for sites with>74 years, although the effect of lime class was not significant ($p=0.144$) (Figure 5b).

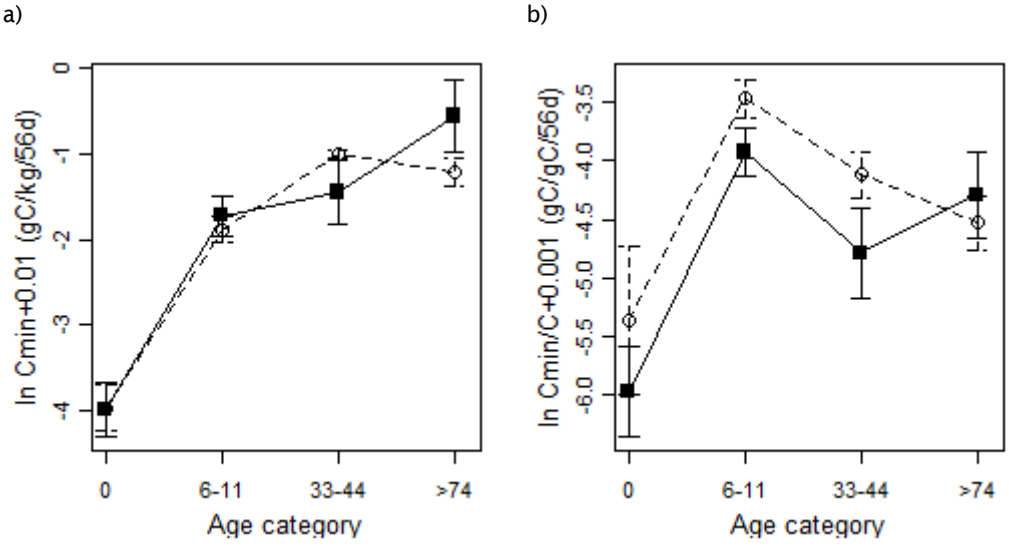

Figure 5. Mean values of a) C mineralization rate and b) C mineralization rate per soil total C for each age category of lime-rich (filled squared) and lime-poor (open circles) sites. Bars indicate standard errors.

To explore the factors influencing the C turnover rate *Cmin/C*, we conducted a series of bivariate regression analyses. *Cmin/C* was highest at intermediate pH (ca. 6-7) (Figure 6a, R^2=0.364, p<0.001, N=40) and at intermediate soil N:C ratio (Figure 6b, R^2=0.675, p<0.001, N=40), and was higher at higher microbial fraction (Figure 6c, R^2=0.681, p<0.001, N=23). Note that soil N:C ratio and soil pH were strongly negatively correlated (Pearson's correlation coefficient r=-0.72, p<0.001). Therefore, the suppressive effects of high pH could be caused by its association with low N:C ratio, and suppressive effects of high N:C ratio could be caused by its association with low pH.
A multivariate regression indicated that the best model (R^2=0.806, p<0.001, N=23) included all three explanatory variables:

$$\ln(Cmin/C+0.001) = -15.1 + 2.8\ pH - 0.2\ pH^2 + 50.4\ soilNC - 617.5\ soilNC^2 + 0.5\ MicC/C$$

Cmin/C reached the optimum at intermediate soil N:C ratio, and under a given soilNC value *Cmin/C* was higher when microbial fraction was higher (Figure 7).

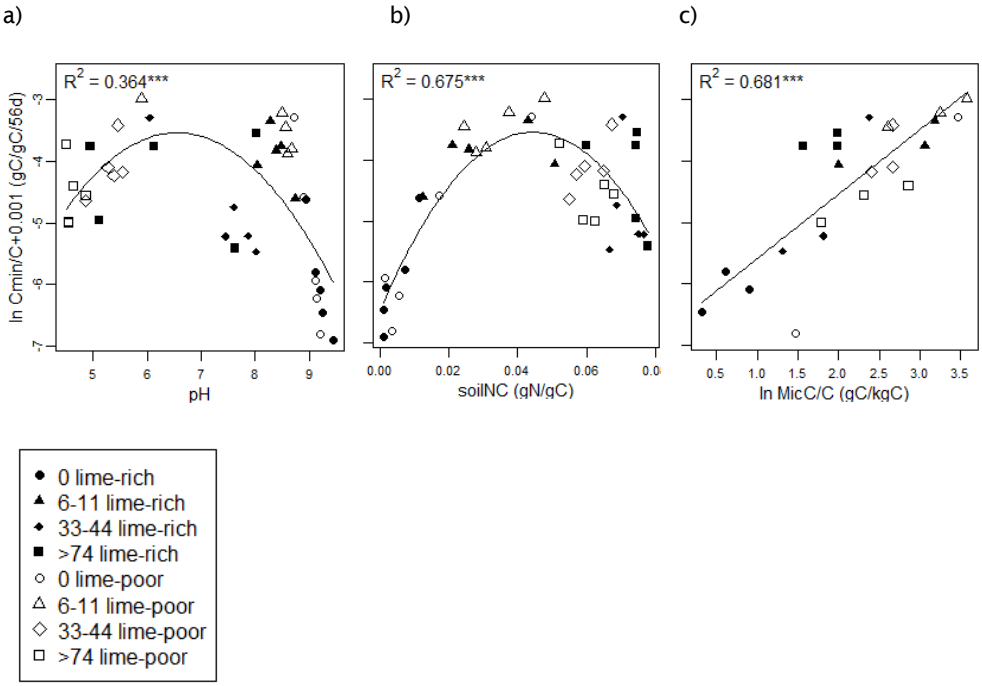

Figure 6. Relationships between C mineralization rate per soil total C and a) soil pH (N=40), b) soil N:C ratio (N=40), and c) microbial fraction (N=23). Bivariate regression models are shown when significant. Different symbols depict the site category (open circles: 0 year & lime-poor, closed circles: 0 year & lime-rich, open triangle: 6-11 years & lime-poor, closed triangle: 6-11 years & lime-rich, open diamond: 33-44 years & lime-poor, closed diamond: 33-44 years & lime-rich, open square: >74 years & lime-poor, closed square: >74 years & lime-rich).

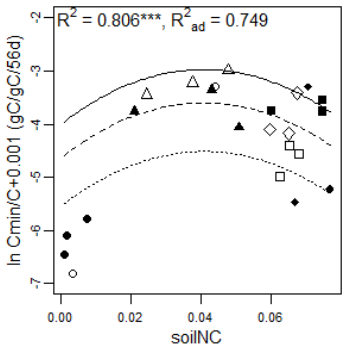

Figure 7. The best model of multivariate regression analysis of C mineralization rate per soil total C regressed by soil pH, soil N:C ratio, and microbial fraction (N=23). The lines show the predicted values of Cmin/C for three different levels of microbial fraction: 95th (solid line), 50th (dashed line), and 5th (dotted line) percentiles of MicC/C, which equal to 32, 10, and 2 gC/kgC, respectively. The median value of Soil pH (8) was used to draw the model. See the caption of Figure 6 for the symbol specifications.

3.1.3. N mineralization rates

N mineralization rates increased with age ($p<0.001$) and were higher in lime-rich sites than lime-poor sites ($p<0.05$) (
Figure 8a). When corrected for soil total C, however, *Nmin/C* was no longer different either among age class ($p>0.05$) or among lime class ($p>0.05$).

Bivariate regression analysis indicated that the effect of soil variables (pH, N:C ratio, and microbial fraction) on *Nmin/C* was similar, though much weaker, to those on *Cmin/C*: pH did not have significant effect on *Nmin/C* anymore (Figure 9a, $p>0.05$); *Nmin/C* reached the highest value at an intermediate *soilNC* level (Figure 9b, $R^2=0.304$, $p<0.01$); and *Nmin/C* increased slightly with increasing *MicC/C* (Figure 9c, $R^2=0.271$, $p<0.05$).

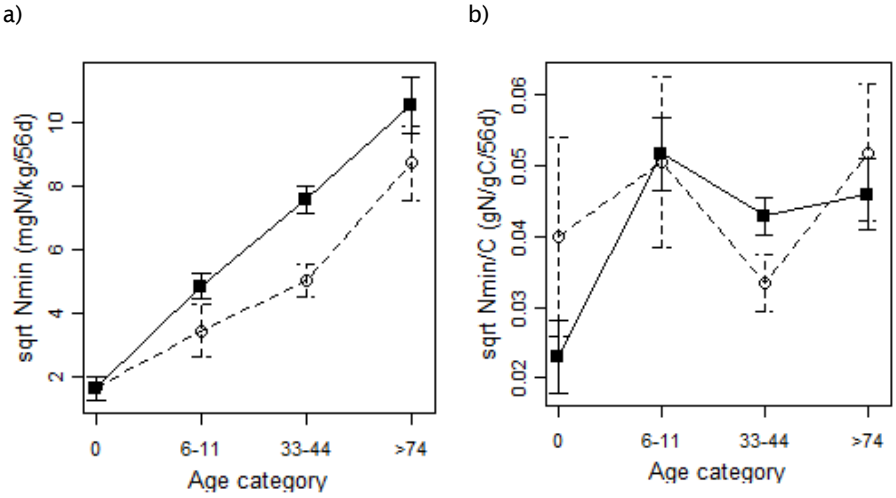

Figure 8. Mean values of a) N mineralization rates and b) N mineralization rate per soil total C for each age category of lime-rich (filled squared) and lime-poor (open circles) sites. Bars indicate standard errors.

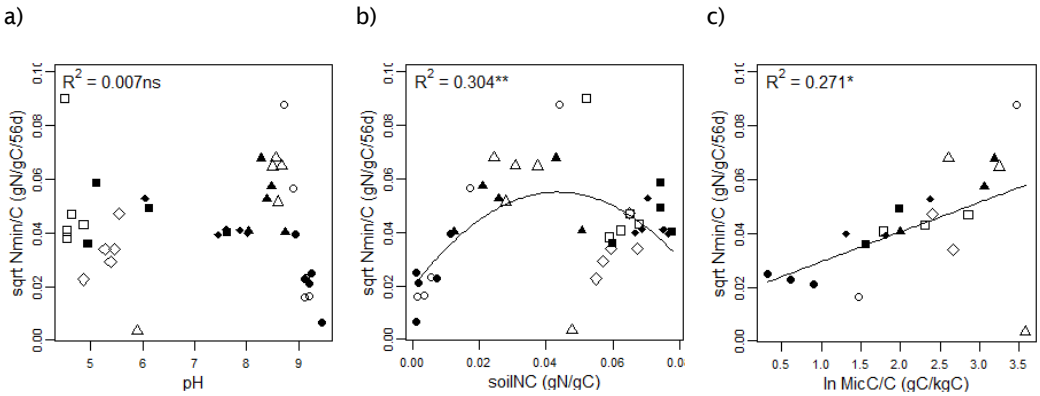

Figure 9. Relationships between N mineralization rate per soil total C and a) soil pH (N=39), b) soil N:C ratio (N=39), and c) microbial fraction (N=22). Bivariate regression models are shown when significant. See the caption of Figure 6 for the symbol specifications.

In order to further explore how N mineralization was regulated, we looked at the ratio between N and C mineralization rates (*Nmin/Cmin*). *Nmin/Cmin* changed with age ($p<0.01$), with a decreasing trend from year 0 to 6_11, and a slightly increasing trend thereafter (Figure 10a). *Nmin/Cmin* was not significantly different between lime class ($p>0.05$), although it was much lower in lime-poor sites at age class 33_44 (Figure 10a). Bivariate regression analysis indicated that *Nmin/Cmin* was the lowest at an intermediate pH (ca. 6-7) (Figure 10b) as well as at an intermediate soil N:C ratio (Figure 10c). Note that, as mentioned earlier, soil N:C ratio and soil pH were strongly negatively correlated. Thus, the observed relationships of *Nmin/Cmin - pH* and *Nmin/Cmin - soilNC* could be confounded each other.

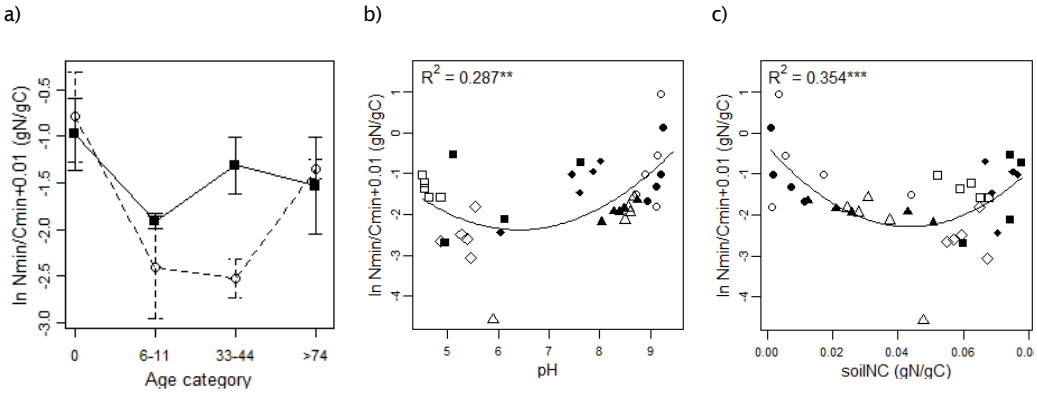

Figure 10. a) Mean values of the ratio of N mineralization rate over C mineralization rate for each age category of lime-rich (filled squared) and lime-poor (open circles) sites. Bars indicate standard errors. b) & c) Relationships between the ratio of N mineralization rate over C mineralization rate and soil pH (b; N=38) and soil N:C ratio (c; N=38). Bivariate regression models are shown when significant. See the caption of Figure 6 for the symbol specifications.

3.2 Vegetation development along succession

3.2.1. Nutrient limitation

Based on the elemental ratio of N, P, and K in biomass, three plots were detected as P-limited or P+N co-limited, and three plots as K-limited or K+N co-limited. These plots did not fall into specific site categories (i.e. P/P+N limited sites were a 33_44-year lime-poor site, a 33_44-year lime-rich site, and a >74-year lime-rich site; K/K+N limited sites were a 6_11-year lime-rich site, a 33_44-year lime-rich site, and a >74-year lime-poor site). In general, however, the plant growth of the majority of the plots was not limited by P (N:P<14.5; Figure 11a) nor by K (N:K <2.1, Figure 11b). Thus, plant growth of dunes in AWD seems to be mainly limited by N (and possibly by other resources, e.g. water availability), irrespective of their exposure to high N deposition in the past. The magnitude of P-limitation relative to N-limitation (i.e. N:P ratio) did not significantly change with age (p>0.05), but was almost significantly (p=0.084) higher for lime-rich sites.

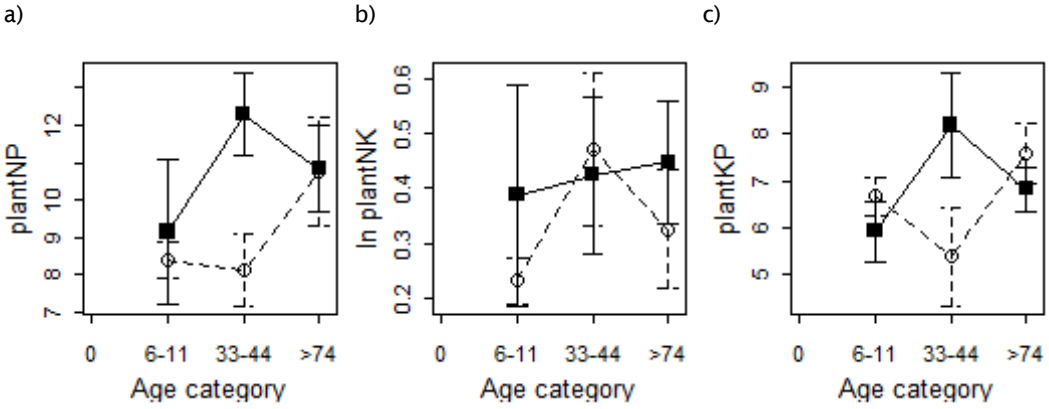

Figure 11. Mean values of a) plant N:P ratio, b) plant N:K ratio, and c) plant K:P ratio for each age category of lime-rich (filled squared) and lime-poor (open circles) sites. Bars indicate standard errors.

3.2.2. Plant biomass

Plant biomass increased with age (p<0.001) and was almost significantly higher for lime-rich sites (p=0.067), although the interaction effect was also significant (p<0.05) (Figure 12). To explore the factors determining the biomass, we conducted regression analyses with soil variables which likely regulate plant biomass; soil pH, N mineralization rate (since N is the limiting nutrient: see the previous section), and gravimetric soil moisture content w_g. Note that w_g was measured only once on a specific moment of April and is merely a rough proxy of soil moisture condition. Bivariate regression analysis showed that plant biomass was highest at an intermediate pH (ca. 6) (R^2=0.558, p<0.001, Figure 13a), and increased with increasing N mineralization rate (R^2=0.601, p<0.001, Figure 13b) and increasing soil moisture (R^2=0.559, p<0.001, Figure 13c). The best model of multivariate regression analysis (R^2=0.672, p<0.001) included soil pH and N mineralization rates as explanatory variables: $\ln(Biomass+10) = -1.93 + 1.83\ pH - 0.146\ pH^2 + 0.386\ \sqrt{Nmin} - 0.019\sqrt{Nmin}^2$.This indicated that plant biomass reached the optimum at an intermediate pH, and under a given pH level a higher N mineralization rate led to a higher plant biomass (Figure 14).

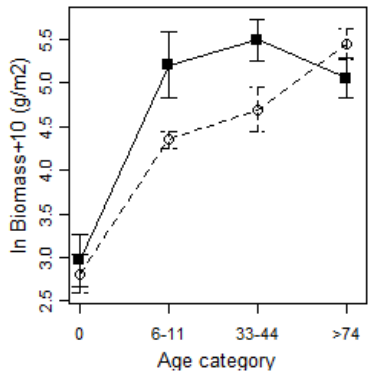

Figure 12. Mean values of above-ground plant biomass for each age category of lime-rich (filled squared) and lime-poor (open circles) sites. Bars indicate standard errors.

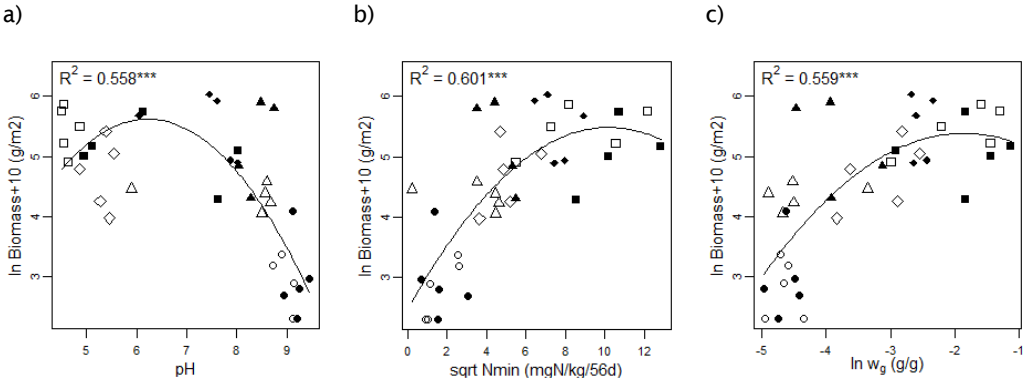

Figure 13. Relationships between above-ground plant biomass and a) soil pH (N=39), b) N mineralization rates (N=38), and c) gravimetric soil moisture (N=39). Bivariate regression models are shown when significant. See the caption of Figure 6 for the symbol specifications.

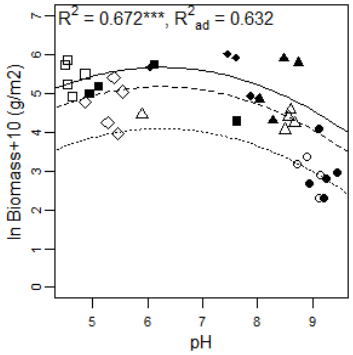

Figure 14. The best model of multivariate regression analysis of plant biomass regressed by soil pH, N mineralization rate, and gravimetric soil moisture (N=38).The lines show the predicted values of biomass for three different levels of N mineralization rates: 95th (solid line), 50th (dashed line), and 5th (dotted line) percentiles of Nmin, which equal to 120, 23, and 0.9 mgN/kg soil/56d, respectively. Gravimetric soil moisture was not selected in the best model.

3.2.3. Plant species diversity

Number of total plant species (i.e. phanerogram, bryophyte, and lichens together) increased with age ($p<0.001$) and was higher for lime-rich sites ($p<0.05$) (Figure 15a). When looking at

phanerogram species only, the species number increases with age too ($p<0.001$) and was much higher for lime-rich sites ($p<0.01$) (Figure 15b). When looking at bryophyte and lichen species only, the trend changed: the species number was much higher for lime-poor sites ($p<0.01$), especially in the age class 33-44 years (interaction effect of age and lime category was significant, $p<0.05$) (Figure 15c).

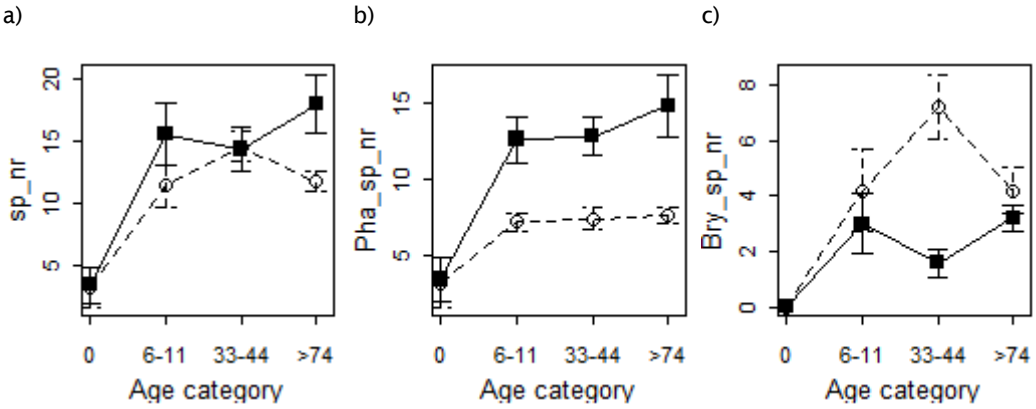

Figure 15. Mean values of a) total plant species number, b) phanerogram species number, and c) bryophyte+lichen species number for each age category of lime-rich (filled squared) and lime-poor (open circles) sites. Bars indicate standard errors.

To explore the factors influencing the species diversity, we conducted regression analysis with variables which likely influence species diversity (i.e. soil pH and plant biomass). The analysis was done separately for phanerogram species and for bryophyte and lichen species. The species diversity of phanerogram was highest at an intermediate pH (ca. 7)(R^2=0.473, $p<0.001$, Figure 16a), whereas that of bryophytes and lichens decreased with pH (R^2=0.369, $p<0.001$, Figure 16b). Species diversity was highest at intermediate plant biomass for both phanerogram (R^2=0.519, $p<0.001$,Figure 16c) and bryophyte+lichen species (R^2=0.329, $p<0.001$,Figure 16d), though the optimum plant biomass was higher for phanerogram species (around 250g/m^2) than bryophyte+lichen species (around 100g/m^2).

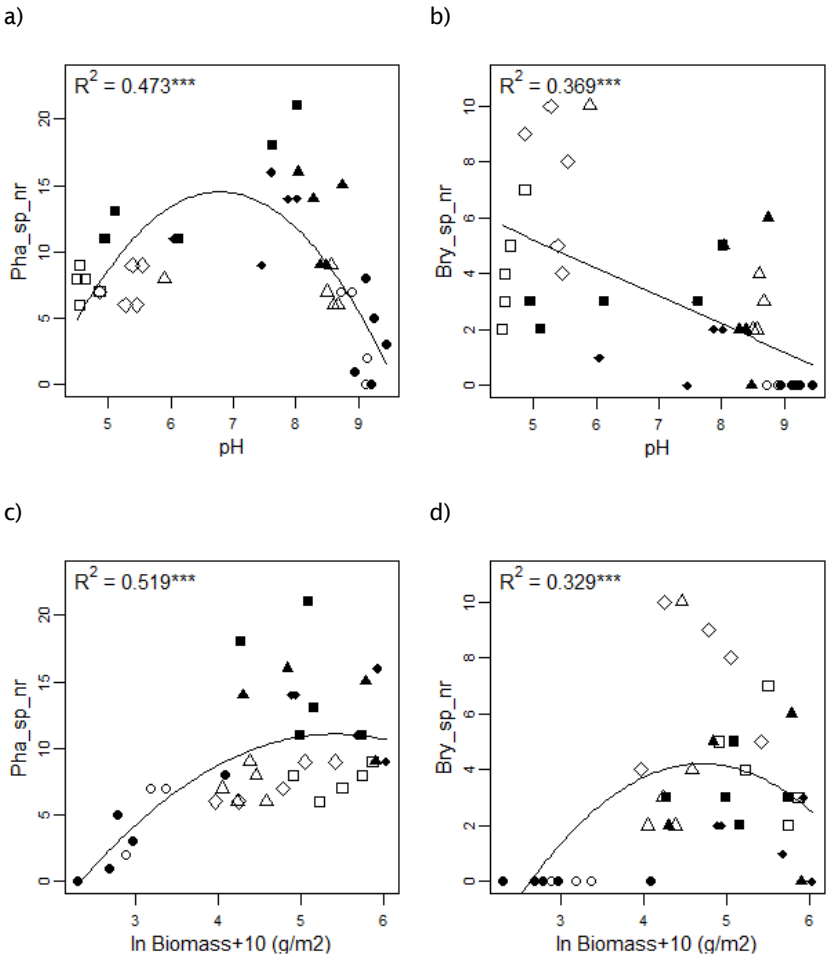

Figure 16. Relationships between a) phanerogram species number vs. soil pH, b) bryophyte+lichen species number vs. soil pH, c) phanerogram species number vs. above-ground plant biomass, and d) bryophyte+lichen species number vs. above-ground plant biomass. Bivariate regression models are shown when significant. See the caption of Figure 6 for the symbol specifications.

3.3 Model simulation

3.3.1. Simulation of dune succession for 3 age classes

Accumulation of soil total C was simulated for 8-year, 38-year, and 75-year succession starting from bare soils (Figure 17). Here we did not include the effect of soil pH nor slope.

The speed of the soil C increase was different among the simulations (Figure 17), reflecting the different levels of atmospheric N deposition during the simulation period: N deposition level was highest from 1970's to 1990's, which corresponds to the 50th to 70th years of 75-year simulation and to the 10th to 30th years of 38-year simulation. The predicted range of soil total C matched reasonably well with the observed value (Figure 17). Note that 0-year sites already have quite some accumulation of soil C in the field, probably due to old SOM from wind-blown eroded soils. These initial soil C (as well as soil N) at age 0 was not considered in our simulation.

The accumulation patterns of soil total N were similar to those of soil total C (Figure 18). The predicted ranges of soil total N, however, were lower than the observed values. The underprediction of the model could be due to absence of N-fixation mechanism in the model.

Plant biomass increases over time, with annual dynamics of growth and death of above-ground biomass. The peak biomass in summer was predicted to level off after a few decades, in accordance with the observation (Figure 19). However, the predicted ranges of plant biomass were too high compared to the observed values. This overestimation of the model could be due to absence of light competition effects for plant growth, due to timing of nutrient uptake by plants (i.e. plant uptake occurs prior to N leaching), or due to a poor representation of water availability in the Century model.

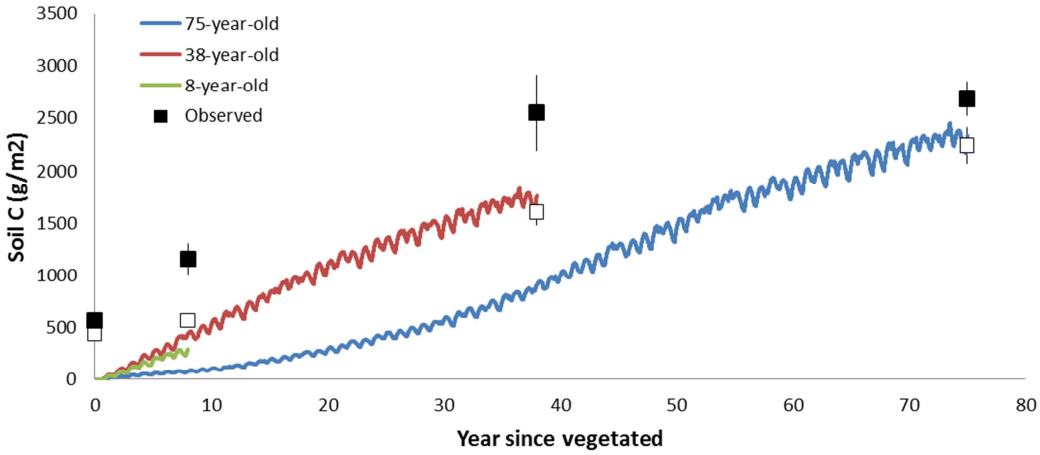

Figure 17. Simulated soil total C for 75-year-old dune (from year 1938 to 2012, blue line), 38-year-oled dune (from year 1975 to 2012, red line), and 8-year-old dune (from year 2005 to 2012, green line). Average and SE values of observed soil total C in 2012 in AWD plots [Aggenbach et al., 2013] are also shown for lime-rich (filled square) and lime-poor (open square) sites (N=5-13) for 0, 6-11, 33-44, and >74 year-old plots.The observed soil total C was calculated as 2xSOM (measured with loss on ignition).

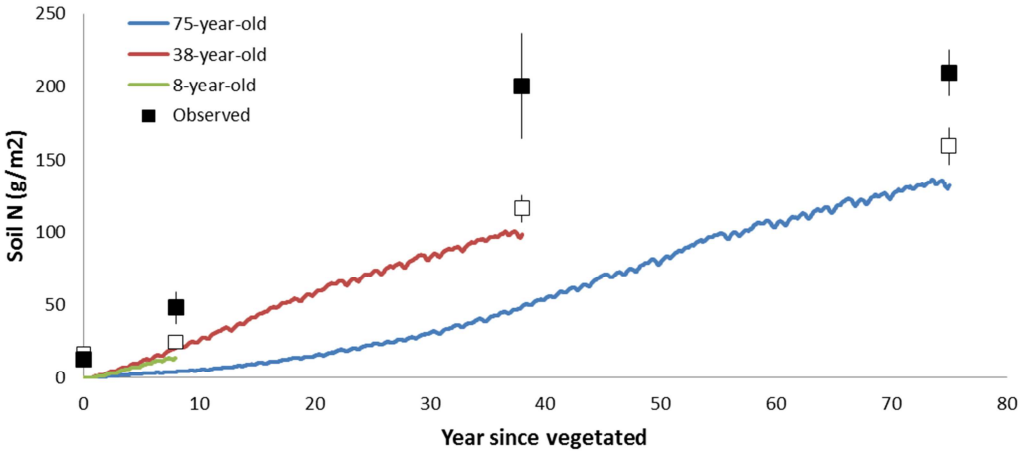

Figure 18. Simulated soil total N for 75-year-old dune (from year 1938 to 2012, blue line), 38-year-oled dune (from year 1975 to 2012, red line), and 8-year-old dune (from year 2005 to 2012, green line). Average and SE values of observed soil total N in 2012 in AWD plots [Aggenbach et al., 2013] are also shown for lime-rich (filled square) and lime-poor (open square) sites (N=5-13).

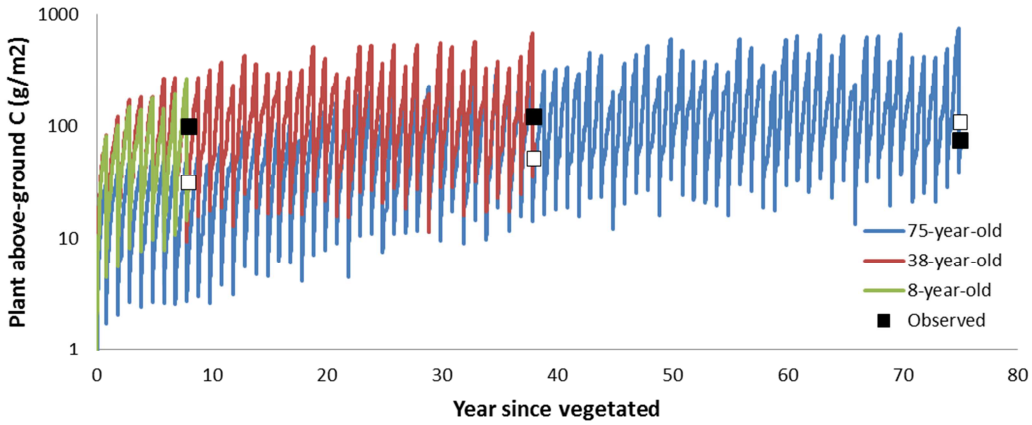

Figure 19. Simulated above-ground biomass of vascular plants for 75-year-old dune (from year 1938 to 2012, blue line), 38-year-oled dune (from year 1975 to 2012, red line), and 8-year-old dune (from year 2005 to 2012, green line). Average and SE values of observed plant biomass in summer 2012 in AWD plots [Aggenbach et al., 2013] are also shown for lime-rich (filled square) and lime-poor (open square) sites (N=5-13).

3.3.2. Simulation of dune succession in lime-rich and lime-poor sites: using Walse *et al.* model

Dune succession for three periods was simulated with the pH effects formulated by *Walse et al.* [1998]. pH values were simulated to decrease from 8.6 (0-year) to 7.2 (8-year), 4.8 (38-year), and 4.0 (75-year) in lime-poor sites, and from 8.3 (0-year) to 7.5 (8-year), 6.2 (38-year), and 5.9 (75-year) in lime-rich sites. Because of the rapid decrease in soil pH in lime-poor sites, the model predicted higher accumulation of soil total C in lime-poor soils than lime-rich soils (Figure 20), which is the opposite pattern to the observation. Thus, the pH effects formulated by *Walse et al.* [1998] are not capable of reflecting the difference in processes between lime-poor and lime-rich sites in AWD.

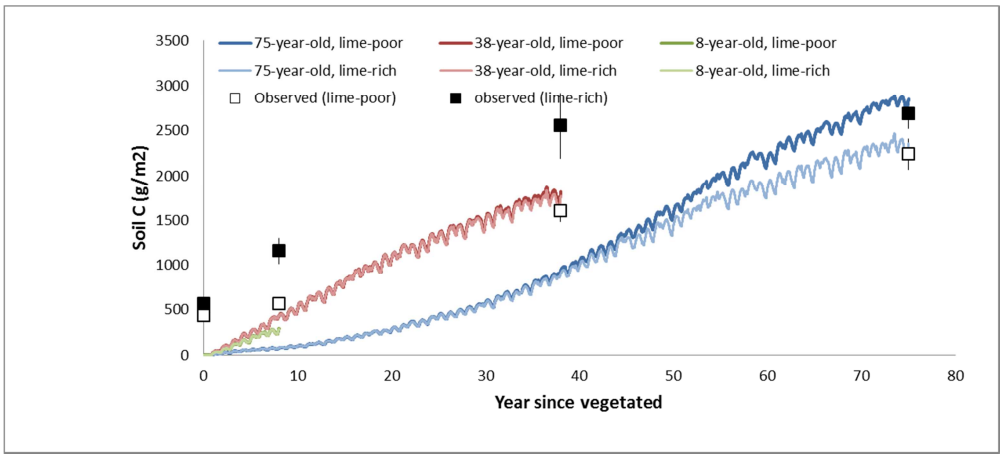

Figure 20. Simulated soil total C for lime-rich and lime-poor sites, for 75-year-old dune (lime-poor: dark blue, lime-rich: light blue), 38-year-oled dune (lime-poor: dark red, lime-rich: light red), and 8-year-old dune (lime-poor: dark green, lime-rich: light green).

3.3.3. Model sensitivity to feedback mechanism of soil physical properties

The impact of including feedback mechanisms of SOM accumulation on soil physical properties (i.e. θ_{sat}) was minor. Accumulation speed of soil total C hardly changed by including the feedback (Figure 21). The virtual absence of the feedback effect was because

θ_{fc}, which is a crucial parameter in the hydrological module to determine the water retention, hardly changed: after 75 years, θ_{fc} increased from 0.140 to 0.143 when the feedback was included (Figure 22). Such a small change in θ_{fc} did not cause any visible changes in the pattern of soil C accumulation.

The predicted small changes of soil physical properties and soil moisture conditions are not consistent with the observations: in the field bulk density decreased and moisture content increased from 0 to >74 years (Figure 13 e&f). The failure of the model in reproducing these trends was mainly caused by the poor estimates of bulk density over time (due to uncertain parameter values in the repro function included in the model).

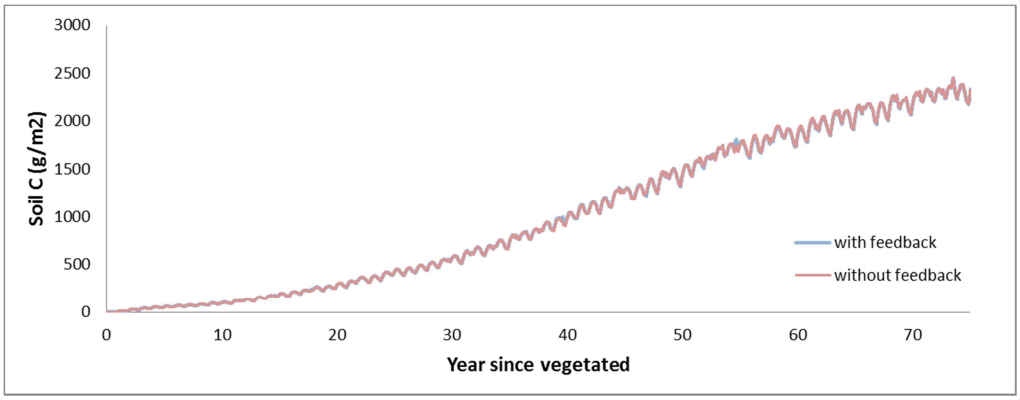

Figure 21. Simulated soil total C for 75 years with (blue) and without (red) feedback mechanisms of SOM accumulation on soil physical properties.

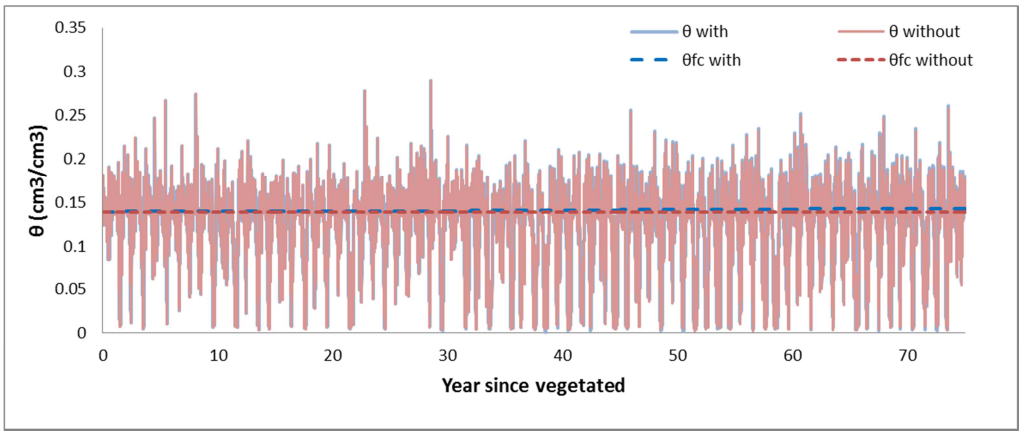

Figure 22. Simulated volumetric water content for 75 years with (blue) and without (red) feedback mechanisms of SOM accumulation on soil physical properties. The volumetric water content at field capacity are also shown (with feedback: dashed blue line, without feedback: dashed red line).

3.3.4. Model sensitivity to slope effects

We simulated soil C accumulation for 75 years for a south slope (30˚ S) and for a north slope (30˚ N). The effects of slope on the simulated C accumulation were almost invisible (Figure 23). However, slope had a significant effect on soil moisture conditions, especially during summer: volumetric water content was lower on the south slope and higher on the North slope, and the difference was large especially in the year with severe dry periods (Figure 24). This effect on soil moisture caused changes in plant growth: predicted plant biomass was higher on the North slope compared to on the South slope (Figure 25). The higher biomass on the North slope was caused by reduced death rate and increased growth rate of plant, both of which are formulated as a function of soil moisture in the model. Note that the

predicted biomass on the North Slope was unrealistically high, due to the inappropriate model formulations (see section 3.3.1).

The predicted little difference in soil total C was in accordance with the field observation: soil total C was not related ($p>0.05$) to the slope factor in any age category (Figure 26 a-c). However, the predicted difference in soil moisture between south and north slopes was not supported by the observation: the observed gravimetric soil moisture content was not related to the slope factor (Figure 26 d-f). Note that the soil moisture was measured in April in the field, whereas the model predicted the large difference in summer periods. Thus, our field data is not appropriate to validate the model prediction. On contrary to the prediction, the observed plant biomass was not related to the slope factor (Figure 26 g-i).

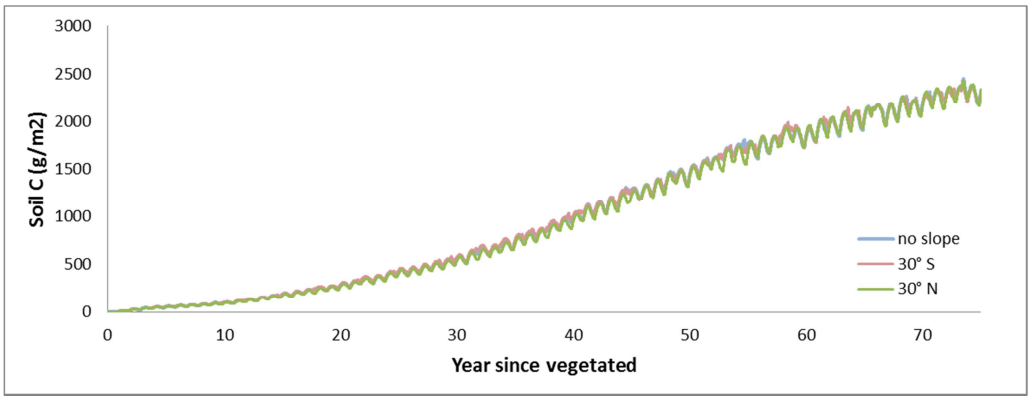

Figure 23. Simulated soil total C for 75 years with no slope effect (blue) and with slope effect (for a south slope of 30˚: red, for a north slope of of 30˚: green).

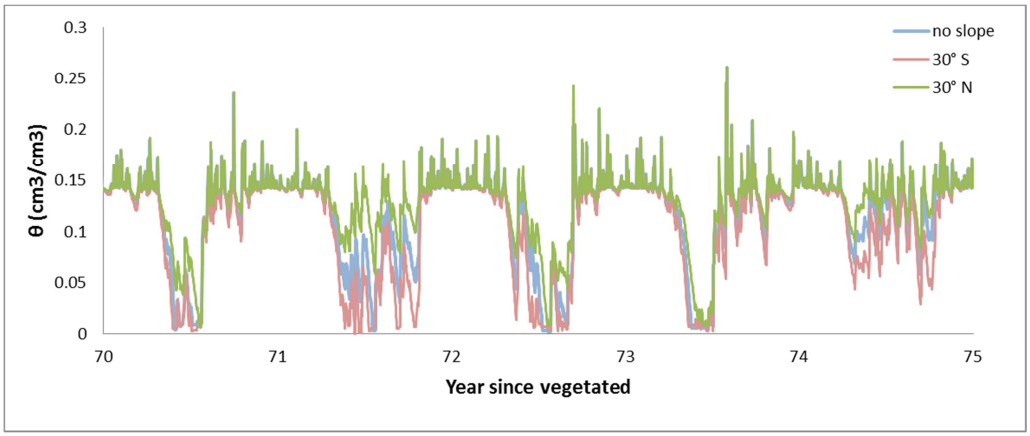

Figure 24. Simulated volumetric water content for 75 years with no slope effect (blue) and with slope effect (for a south slope of 30˚: red, for a north slope of of 30˚: green). The values between 70th and 75th years are shown.

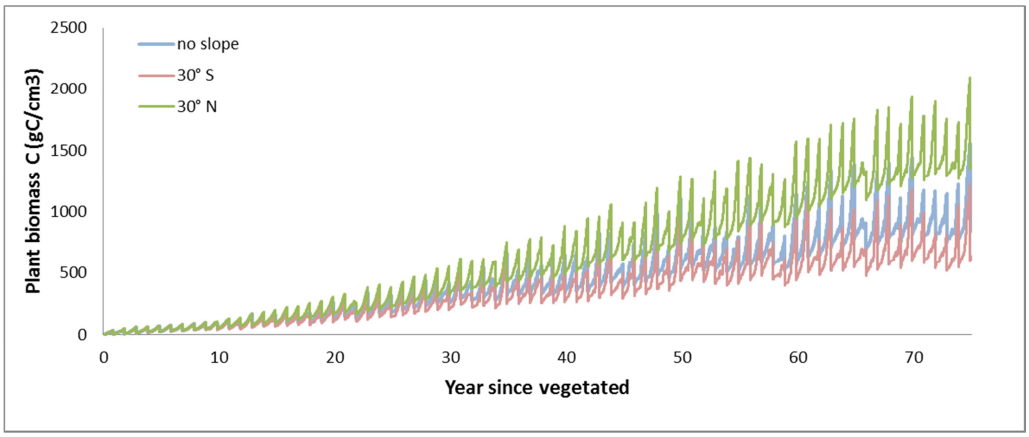

Figure 25. Simulated above-ground plant biomass for 75 years with no slope effect (blue) and with slope effect (for a south slope of 30°: red, for a north slope of of 30°: green).

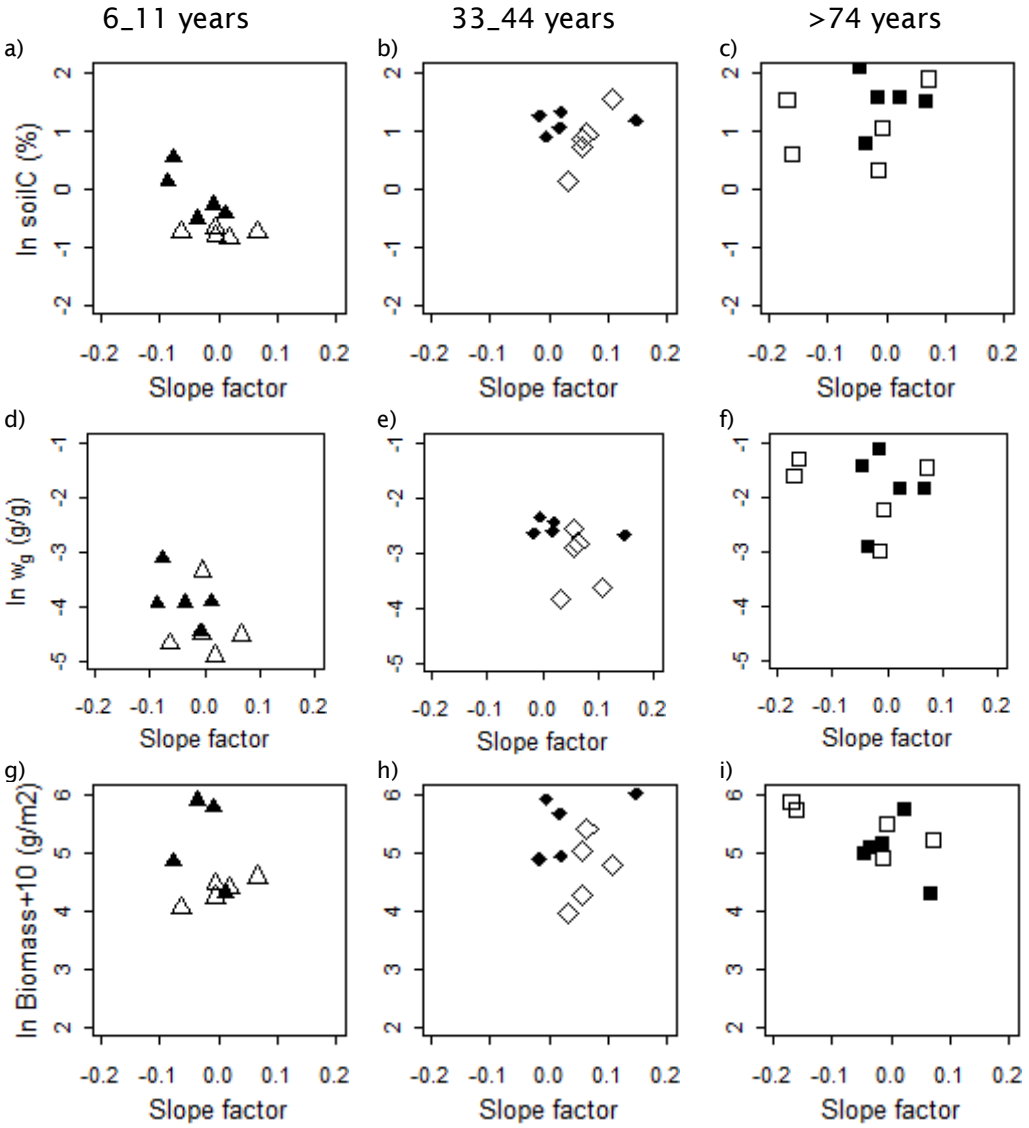

Figure 26. Effects of slope on observed data of a)-c) soil total C, d)-f) gravimetric moisture content, and g)-i) above-ground plant biomass. Each age category is shown separately (left: 6_11 years, middle: 33_44 years, right: >74 years). Open symbols depict lime-poor sites, whereas closed symbols depict lime-rich sites. Effect of slope was expressed as slope factor f_{SLP}, which was computed from the aspect and angle of the slope (see Method section 2.6.1). For none of the age categories and for none of the response variables, f_{SLP} had significant ($p<0.05$) effect.

4 Discussion and conclusions

4.1. Factors influencing SOM turnover and accumulation

In accordance with the previous study in the same area [*Aggenbach et al.*, 2013], the speed of SOM accumulation was faster in lime-rich than in lime-poor sites. The faster accumulation of SOM in lime-rich site coincides with slightly slower C turnover rate (i.e. *Cmin/C*) in lime-rich sites.

Our study identified several potential soil factors which influence C turnover rates. Fraction of microbial C in soil total C seemed to be the most influential factor determining C turnover rate: it explained ca. 68% of variation in *Cmin/C*. The importance of microbial pool size on C turnover rate was also pointed out in a global study [*Fujita et al.*, in revision]. This positive relationship between C turnover rate and microbial fraction explains the slower C turnover rate of lime-rich sites, since lime-rich sites had significantly lower microbial fraction than lime-poor sites in our study. This trend, however, is not supported by another study in AWD showing that microbial fraction did not differ between lime-rich and lime-poor sites (Kooijman et al. *in prep*). Our study used SIR method, which is a simple but an indirect method to estimate microbial C, instead of more reliable fumigation method. Also, we did not directly measure microbial activity, whereas it is generally known that a number of factors (soil moisture, pH, substrate quality, microbial composition) influence the microbial efficiency in decomposing C ([*Keiblinger et al.*, 2010; *Manzoni et al.*, 2012; *Sinsabaugh et al.*, 2013]). Thus, more detailed measurements on microbial characteristics will be needed to further investigate if and how the difference in microbial community influence C turnover rates in lime-rich and lime-poor sites.

In addition to the effect of microbial fraction, soil N:C ratio had significant influence on C turnover rates: C turnover rate was suppressed by low soil N:C ratio in early successional stage. The negative effects of N richness on C decomposition has been indicated both empirically [*Manzoni et al.*, 2008; *Parton et al.*, 2007] and theoretically [*Manzoni and Porporato*, 2007; *Porporato et al.*, 2003]. In our study, however, soil N:C ratio was not different between lime-rich and lime-poor sites in early succession stage. This could be related to almost identical pH levels in lime-rich and lime-poor sites in the early successional stage. Thus, soil N:C ratio was not an extra factor explaining the difference in C turnover rate between lime-rich and lime-poor sites.

Moreover, although the relationship was rather weak, C turnover rate was also related to soil pH: low pH suppressed C turnover rate in later successional stage. Low pH is known to negatively influence microbial activity due to associated aluminium toxicity [*Walse et al.*, 1998], and the negative relationships between soil pH and decomposition were evident in previous studies [*Aciego Pietri and Brookes*, 2008; *Walse et al.*, 1998]. Moreover, lime content could indirectly influence SOM decomposition via forming Ca-SOM complexes which inhibit decomposition. Although pH per se did not explain the difference in *Cmin/C* between lime-poor and lime-rich sites over all age classes in out study, pH did help explaining the pattern in the oldest age (>74 years): the similar *Cmin/C* between lime class irrespective of slightly higher microbial fraction in lime-poor sites in this age category was probably due to much lower pH in lime-poor sites.

4.2. Factors influencing N availability

Factors influencing N mineralization are more complex than that for C mineralization. In general, C mineralization rate and N mineralization rate are strongly correlated because these processes are closely coupled by decomposition activity of microbes. However, the relationships can deviate depending on several soil factors, such as stoichiometry (i.e. C:N ratio) of soil substrate and microbes, as well as physiological characteristics of microbial community. Using the equations of CENTURY, the ratios of *Cmin* and *Nmin* can be expressed as follows

$$\frac{Nmin}{Cmin} = \frac{NC_S - e \cdot NC_M}{1 - e}$$

where NC_S is the N:C ratio of soil substrate, e is the microbial yield efficiency, and NC_M is the N:C ratio of microbes. This means that, in theory, the ratio of *Nmin* to *Cmin* increases with increasing soil N:C ratio and decreasing microbial N:C ratio. Moreover, under the condition of $NC_S < NC_M$ (which is generally the case), *Nmin/Cmin* decreases with increasing *e*.

With our data, *Nmin/Cmin* increases with successional age after 6_11 years, which coincides with an increase in soil N:C ratio and therefore is consistent with the above-mentioned theory. The increase in *Nmin/Cmin* in later successional stage may also be related to decreasing soil pH, as soil pH is an indirect proxy for microbial N:C ratio (i.e. acid soils are often, though not always, dominated by fungi rather than bacteria [*Strickland and Rousk*, 2010] and fungi usually have lower N:C ratio than bacteria [*Six et al.*, 2006]). A significantly lower microbial N:C ratio in lime-poor (i.e. low pH) than in lime-rich sites was also observed in a study in AWD (Kooijman et al. unpublished). Thus, although not explicitly measured in our study, increasing substrate N:C ratio and decreasing microbial N:C ratio along succession seems to explain the increase in N mineralization rates relative to C mineralization rates.
We don't have a clear explanation why *Nmin/Cmin* was higher at age 0, where soil substrate N:C ratio was low and soil pH was high. It is likely that both *Cmin* and *Nmin* were very low in this age category and therefore the measurement error in the ratio was large. An alternative explanation could be that microbial yield efficiency, which was not measured in our study, plays a role here: microbial yield efficiency is low when substrate quality (e.g. decomposability of C) is low [*Manzoni et al.*, 2008], and lower yield efficiency would in theory lead to higher *Nmin/Cmin*.

The difference in *Nmin/C* between lime-rich and lime-poor sites was less apparent than that in *Cmin/C*; slightly higher *Cmin/C* in lime-poor sites was mitigated by slightly lower Nmin/Cmin in these sites, resulting in similar Nmin/C in both lime classes. N turnover rate (i.e. *Nmin/N*) was also indifferent between lime-rich and lime-poor sites. This probably explains why N accumulation rates were not different between lime classes. This leads to the observed pattern that total N mineralization rates per gram soil were higher for lime-rich sites: because soil total N was higher for lime-rich soils and N mineralization rates per N was indifferent between lime classes. This is, however, an opposite pattern found in the previous studies which showed higher N mineralization rates in acid than calcaric soils [*Kooijman and Besse*, 2002; *Kooijman et al.*, 2008]

4.3. Factors influencing plant productivity and species diversity

Plant peak standing crop was higher in lime-rich sites than in lime-poor sites, except for the young (0 year) and latest (>74 years) successional stage. This is in accordance with the results of *Kooijman and Besse* [2002] in AWD that biomass production was higher in slightly decalcified than fully decalcified dunes, peaking around pH 5-6. In our study, the higher plant biomass production in lime-rich sites was explained by higher N mineralization rates in lime-rich sites in the intermediate successional stages. At the latest successional stage, soil

pH drops and suppresses plant production. It is not clear why the decrease in plant production in the latest age was severer in lime-rich sites where the pH drop was smaller.

Biodiversity of total plant species was higher for lime-rich soils. Interestingly, the factors influencing species diversity were different between plant functional groups; phanerogams were suppressed by low pH whereas bryophyte + lichens had the highest diversity at relatively low pH (ca. 5-6); diversity of phanerogram was not suppressed by plant biomass (at least in the range of the biomass observed in our study) whereas that of bryophyte + lichens was slightly suppressed when plant biomass exceeds ca. 100 g/m^2. As a result, bryophyte + lichen species were richer in lime-poor sites and phanerogram species were richer in lime-rich sites. This means that higher N mineralization rates in lime-rich sites (which resulted in higher plant biomass) did not lead to lower biodiversity, indicating that higher N availability per se (whether by soil mineralization or atmospheric N deposition) is not necessarily an immediate threat for diversity loss in this ecosystem. However our data set was collected in the low range of the productivity gradient of dune grasslands, because productive grasslands with a strong grass encroachment were excluded during plot selection. Therefore we were probably not able to detect a negetative effect of standing crop on species diversity. Because soil pH has a strong effect on species diversity, the factors determining the speed of pH decrease with successional age needs to receive more attention to understand the mechanism of diversity decline along successional stage. Note that we did not analyze the species composition of each plot and how it shifts with changing soil nutrient and acidity conditions. More careful examination of occurrence of individual species (especially vulnerable species and species with high conservation values) is needed to make further suggestions.

Despite of the high level of atmospheric N deposition in last decades, growth of phanerogams in all sites seems to be primarily limited by N. This could be because soil P availability is relatively high in the dune ecosystmes of this region [*Kooijman et al.*, 1998]. Soil P availability, however, plays a more important role in limiting plant growth in lime-rich sites. In order to conserve plant diversity in dune ecosystems, it is important to consider soil P availability as well as the geochemical factors controlling the P availability [*Kooijman et al.*, 1998; *Kooijman et al.*, 2009]. Moreover, we did not examine the nutrient status of moss and lichen species, despite that these species contributed to a large part of plant biomass for some plots. The influence of N and P availability on mosses and lichens as well as their feedback to the nutrient cycles could be different from those of phanerograms and may play an important role. Future studies are needed to explicitly consider mosses and lichens in nutrient dynamics of dune ecosystems.

4.4. Long-term prediction of dune succession: which aspects of the model should be further improved?

Our simple model made reasonable predictions of soil C accumulation of long-term dune succession. The level of atmospheric N deposition in the past had strong effects on the current SOM level, as well as on nutrient availability and plant production. This implies that high N deposition level speeds up dune succession, and therefore time-scale of the nature management in dune ecosystems. Although we used national average levels of N deposition as input values, spatial heterogeneity of N deposition within AWD is known to be high. E.g. N deposition level tends to be lower in lime-rich than lime-poor sites, because of the spatial gradient in lime content is opposite to the gradient of N-deposition (Aggenbach 2013 *pers.comm.*). To further test the impact of N deposition on SOM dynamics, future studies are needed with finer-scale N deposition records in the past as well as observation data of topograpiclly contrasting dune sites.

In contrast to the reasonably good prediction for soil C, our model did a much poorer job for soil N and plant production. Moreover, the difference between lime-poor and lime-rich sites could not be properly reconstructed. In order to improve the model predictions, model

formulations of several processes should be re-examined. First, the model output was very sensitive to the equations of plant growth, nutrient leaching, as well as the timing and order of these processes to occur. Sensitivity analysis will help understanding the impact of these parameter values on model outputs, and quantifying the propagation of the uncertainty associated with them.

Second, the hydrology of the dune soils should be better represented in the model. The hydrological module of the CENTURY model is rather simple, and our small modifications on the module (i.e. feedback of SOM accumulation on soil physical properties, slope effects on evapotranspiration) was not enough to reproduce the observed patterns of soil moisture in the field. The formulations of the SOM feedback and the slope effect used in this study were based on empirically-derived repro functions from different ecosystems. Thus, more ecosystem-specific dataset for dunes will help reducing the uncertainty in the repro functions and therefore improve the model performance. Moreover, better understanding on the mechanisms, better schematization of soil characteristics, as well as more rigor validation of the model output are necessary to make a step forward.

Third, more processes which are crucial in dry dune systems should be explicitly included in the model. Recent studies showed that the patterns of evapotranspiration were different in bare and moss-dominated soils compared to more vegetated soils, both in the lab [*Voortman et al.*, in prep.] and in field conditions [BTO project 'Meetsysteem actuele verdamping' (B111800)]. Such vegetation-type-specific patterns of hydrological processes may play an important role in regulating SOM accumulation, especially in the early phase of dune succession, and therefore should be incorporated in the model. Also, a better formulation of the soil moisture effects on plant performance is needed. Soil moisture effects on plant growth is now included in a very simple manner, without being able to reflect the soil-specific impact of a certain water content in soils. This should be replaced by more process-based formulation, such as 'drought stress' [*Bartholomeus et al.*, 2008] (although it needs to be verified and validated for the dune ecosystems before being applied). Moreover, the simple formulation of pH effects that we incorporated in this study was not enough to reconstruct the observed patterns in lime-rich and lime-poor sites. Also, the change in pH over time was approximated by a simple empiricaly-based reprofunctions, whereas in reality soil pH is regulated in complicated processes (e.g. amount of SOM and base status influence buffering capacity of soils). More process-based understanding on the decomposition processes, especially those related to microbial activity and biogeochemistry of soil, will help to capture the site-specific processes in the model.

Finally, more efforts are needed to validate the model outputs with observed data, for different elements of ecosystems (e.g. soil moisture, plant growth, soil C) separately. More dataset including different successional stage and lime classes, such as those of this study and of *Aggenbach et al.* [2013], will be required for such validation studies. Also more data of the more productive dune grasslands should be included. More accurate measurements of plant productivy instead of standing crop (influenced by grazing) provide a better check for modelled productivity. Also, more detailed dataset of microbial properties and activity will help improving small-scale processes of decomposition and making the model more robust to changing environmental conditions.

4.5. Summary of findings

- Research aim 1 (results presented in chapter 3.1): to examine factors differentiating the SOM accumulation rates between lime-poor and lime-rich dunes
    - Accumulation speed of soil C was slower in lime-poor than lime-rich sites. This is, at least partly, due to faster C turnover rate in lime-poor sites, caused by their higher abundance of microbes. However, as succession goes on, pH drops rapidly in lime-poor sites and suppresses decomposition rates. This makes the

difference in C turnover rates between lime classes to diminish in the late successional stage.

  - Accumulation speed of soil N was not different between lime-rich and lime-poor sites, and was determined by complex processes. In addition to the factors influencing C decomposition, stoichiometry of soil substrate and microbes, as well as microbial physical characteristics also played a role in determining the N turnover rate.

- Research aim 2 (results presented in chapter 3.2): To examine factors differentiating plant biomass and species richness between lime-poor and lime-rich dunes

  - N mineralization rate was higher in lime-rich than lime-poor sites, because of high soil N content rather than high N turnover rate. This leads to higher plant biomass production in lime-rich sites (at least in intermediate successional stages).

  - Plant diversity was slightly higher in lime-rich sites. Phanerogram species were richer in lime-rich sites because low pH had negative impacts on this group of species. Bryophyte and lichen species were richer in lime-poor sites because these species were not suppressed by relatively low pH and because moderately high plant biomass in lime-rich sites already suppresses these group of species.

- Research aim 3 (results presented in chapter 3.3): To understand the long-term development of dune soils and vegetation, by developing a process-based model of soil, water, and vegetation and by validating the model for lime-poor and lime-rich dunes

  - With the modified CENTURY model that couples SOM, hydrology, and vegetation, C accumulation of dune succession was predicted reasonably well, but N accumulation and plant production was predicted less accurately. The observed patterns of the effects of lime richness and slope were poorly predicted by the model. This highlights the needs for further improvement of the model.

- This study increased our understanding on how N availability for plants is regulated in lime-poor and lime-rich dune ecosystems. This helps improving PROBE, the model to predict vegetation types for nature conservation purpose.

4.6. Implication for nature management

The results of this study have implications for the planning of restoration measures and vegetation management. These implications are related to the (potential) effects of restoration measures listed by Smits and Kooijman (2012a+b) for grey dunes degraded by N-deposition (appendix IV). Partly these implications are hypothetical and therefore it is not possible to present precise restoration guidelines. In genera, it is important to include both measures with short-term (e.g. mowing, grazing) and long term (e.g. sod cutting, excavation, promoting large scale eolian activity) restoration effects in management plans.

A high atmospheric N deposition in the past led to a stronger increase of the C and N pool in soil and therefore also currently led to a higher N mineralization rate. Removal of top soil where most of the SOM and N-pool is located will help decreasing N availability for Phanerogam plants. Because most dune grasslands are N-limited removal of the SOM pool by top soil excavation, sod cutting or soil renewal by aeolian dynamics is very effective to lower plant productivity. These measures are indicated as potentially very effective in the restoration strategy for grey dunes (Smits & Kooijman a+b). However these measures will

promote restoration of species-rich grey dunes 2-3 decades after the measure because species-rich grey dunes depend on a humus profile (Aggenbach et al. 2013). Therefore complete SOM removal or renewal of SOM-poor sand soils is only applicable in restoration strategies planned on a longer term. Less severe measures for topsoil removal (shallow sod cutting, removing litter layer by choppering) remove less of the N-pool and subsequently lower the N-mineralisation to a lesser extent. The plant productivity after these measures depends on the remaining SOM-pool and mineralisation rate. Restoration of grey dune vegetation may be faster if a humus profile, underground parts of plants and the seed bank still remains. Removing the aboveground vegetation and litter layer with a special equipment (dutch: kleppelen+afzuigen = sprangelen; diep maaien met maaizuigcombi) may have a relatively long positive effect after the measure if the removed litter layer contributed much to the total N-mineralisation.

In older soils extra accumulation of SOM due to a high N-deposition in the past may limit the effectiveness of measures which do not remove the major part of the N-pool. The effects and sustainability of these measures may therefore also depend on the SOM pool. Measures which remove the above ground vegetation (mowing, grazing, burning) have a fast positive effect on grey dune vegetation because of improved light condition (lower herb and less dense layer). Our results indicate mosses and lichens may profit from less aboveground standing crop. In case of removing above ground biomass and litter especially mosses and lichens of the Festuco-Galietum profit, while in case of removing also the humus horizon often species of Violo-Corynephoretum are enhanced (communication Mark van Til). However, grazing not always decreases grass cover and promotes mosses and lichens. In some areas, like Harstenhoek in Meijendel, grazing with ponies induced the opposite development (Van der Hagen 2011). Grazing pressure and the type of grazers may be important factors for the effects on functional plant groups and vegetation structure.

The current and future N-deposition will also influence the impact of restoration measures because the level of N-deposition influences SOM accumulation. At a high level of N-deposition (much more than the critical load) the development a humus profile and grey dune vegetation will be faster because the productivity of the vegetation and therefore accumulation of soil organic matter is often limited by nitrogen. This may have consequences for the sustainability of species-rich grey dunes after secondary succession promoted by restoration measures.

Finally, the species richness of Phanerogam is strongly influenced by pH. Measures which improve the base status of strongly acidified grasslands will have a positive effect on many typical phanerogams. The effectiveness of such measures depends strongly on the decalcification profile. Management plans should therefore also focus on recovery of the base status, which can be achieved by restoration of the wind dynamics (new base rich soils, input of base rich sand in existing dune grasslands) or artificial addition of acid buffer capacity (e.g. scatering of lime rich sand in acidified dune grasslands).

5 Literature

Aciego Pietri, J. C., and P. C. Brookes (2008), Nitrogen mineralisation along a pH gradient of a silty loam UK soil, *Soil Biology and Biochemistry*, *40*(3), 797-802.

Aggenbach, C. J. S., A. M. Kooijman, R. P. Bartholomeus, and Y. Fujita (2013), Herstelbaarheid van droge duingraslanden in relatie tot accumulatie van organische stof en stikstof in de bodem, *KWR 2013.028*, 73 pp, KWR Watercycle Research Institute.

Anderson, J. P. E., and K. H. Domsch (1978), A physiological method for the quantitative measurement of microbial biomass in soils, *Soil Biology and Biochemistry*, *10*(3), 215-221.

Bartholomeus, R. P., J. P. M. Witte, P. M. van Bodegom, J. C. van Dam, and R. Aerts (2008), Critical soil conditions for oxygen stress to plant roots: Substituting the Feddes-function by a process-based model, *Journal of Hydrology*, *360*(1-4), 147-165.

Bettinelli, M., U. Baroni, and N. Pastorelli (1989), Microwave oven samle dissolution for the analysis of environmental and biological materials, *Analytica Chimica Acta*, *225*(0), 159-174.

Bobbink, R., et al. (2010), Global assessment of nitrogen deposition effects on terrestrial plant diversity: A synthesis, *Ecological Applications*, *20*(1), 30-59.

Del Grosso, S., D. Ojima, W. Parton, A. Mosier, G. Peterson, and D. Schimel (2002), Simulated effects of dryland cropping intensification on soil organic matter and greenhouse gas exchanges using the DAYCENT ecosystem model, *Environmental pollution*, *116*(SUPPL. 1), S75-S83.

Del Grosso, S. J., W. J. Parton, A. R. Mosier, D. S. Ojima, A. E. Kulmala, and S. Phongpan (2000), General model for N2O and N2 gas emissions from soils due to dentrification, *Global Biogeochemical Cycles*, *14*(4), 1045-1060.

Fujita, Y., P. M. van Bodegom, H. Olde Venterink, H. Runhaar, and J.-P. M. Witte (2013), Towards a proper integration of hydrology in predicting soil nitrogen mineralization rates along natural moisture gradients, *Soil Biology and Biochemistry*, *58*(0), 302-312.

Fujita, Y., J. P. M. Witte, and P. van Bodegom (in revision), Incorporating microbial ecology concepts into soil mineralization models to improve regional predictions of carbon and nitrogen fluxes.

Heinen, M. (2006), Application of a widely used denitrification model to Dutch data sets, *Geoderma*, *133*(3-4), 464-473.

Jansen, P. C., and J. Runhaar (2005), Toetsing van het verband tussen het aandeel xerofyten en de droogtestress onder verschillende omstandigheden, *Alterra-rapport 1045*, 74 pp, Alterra, Wageningen.

Jones, M. L. M., A. Sowerby, D. L. Williams, and R. E. Jones (2008), Factors controlling soil development in sand dunes: Evidence from a coastal dune soil chronosequence, *Plant and Soil*, *307*(1-2), 219-234.

Keiblinger, K. M., et al. (2010), The effect of resource quantity and resource stoichiometry on microbial carbon-use-efficiency, *FEMS Microbiology Ecology*, *73*(3), 430-440.

Kooijman, A., H. Van Der Hagen, and E. Noordijk (2012), Stikstof depositie in de duinen: alles in beeld?, *Landschap*, *29*(3), 147-154.

Kooijman, A. M., J. C. R. Dopheide, J. Sevink, I. Takken, and J. M. Verstraten (1998), Nutrient limitations and their implications on the effects of atmospheric deposition in coastal dunes; lime-poor and lime-rich sites in the Netherlands, *Journal of Ecology*, *86*(3), 511-526.

Kooijman, A. M., and M. Besse (2002), The Higher availability of N and P in lime-poor than in lime-rich coastal dunes in the Netherlands, *Journal of Ecology*, *90*, 394-403.

Kooijman, A. M., M. M. Kooijman-Schouten, and G. B. Martinez-Hernandez (2008), Alternative strategies to sustain N-fertility in acid and calcaric beech forests: Low microbial N-demand versus high biological activity, *Basic and applied ecology*, *9*(4), 410-421.

Kooijman, A. M., I. Lubbers, and M. van Til (2009), Iron-rich dune grasslands: Relations between soil organic matter and sorption of Fe and P, *Environmental pollution*, *157*(11), 3158-3165.

Manzoni, S., and A. Porporato (2007), A theoretical analysis of nonlinearities and feedbacks in soil carbon and nitrogen cycles, *Soil Biology and Biochemistry*, *39*(7), 1542-1556.

Manzoni, S., R. B. Jackson, J. A. Trofymow, and A. Porporato (2008), The global stoichiometry of litter nitrogen mineralization, *Science*, *321*(5889), 684-686.

Manzoni, S., P. Taylor, A. Richter, A. Porporato, and G. I. Ågren (2012), Environmental and stoichiometric controls on microbial carbon-use efficiency in soils, *New Phytologist*, *196*(1), 79-91.

Metherell, A. K., L. A. Harding, C. V. Cole, and W. J. Parton (1993), *CENTURY soil organic matter model environment. Technical documentation agroecosystem version 4.0.*, 247 pp.

Moldrup, P., T. Olesen, J. Gamst, P. SchjÃ¸nning, T. Yamaguchi, and D. E. Rolston (2000), Predicting the gas diffusion coefficient in repacked soil: Water-induced linear reduction model, *Soil Science Society of America Journal*, *64*(5), 1588-1594.

Noordijk, H. (2007), Nitrogen in the Netherlands over the past fivecenturies, paper presented at First International Ammonia Conference in Agriculture, Ede, Nederland.

Olde Venterink, H., M. J. Wassen, A. W. M. Verkroost, and P. C. de Ruiter (2003), Species richness-productivity patterns differ between N-, P-, and K- limited wetlands, *Ecology*, *84*(8), 2191-2199.

Parton, W., et al. (2007), Global-scale similarities in nitrogen release patterns during long-term decomposition, *Science*, *315*(5810), 361-364.

Parton, W. J., D. S. Schimel, C. V. Cole, and D. S. Ojima (1987), Analysis of Factors Controlling Soil Organic-Matter Levels in Great-Plains Grasslands, *Soil Science Society of America Journal*, *51*(5), 1173-1179.

Parton, W. J., et al. (1993), Observations and modeling of biomass and soil organic matter dynamics for the grassland biome worldwide, *Global Biogeochemical Cycles*, *7*(4), 785-809.

Porporato, A., P. D'Odorico, F. Laio, and I. Rodriguez-Iturbe (2003), Hydrologic controls on soil carbon and nitrogen cycles. I. Modeling scheme, *Advances in Water Resources*, *26*(1), 45-58.

R Development Core Team (2013), R: A language and environment for statistical computing. R Foundation for Statistical Computing, Vienna, Austria. URL http://www.R-project.org/. edited.

Sinsabaugh, R. L., S. Manzoni, D. L. Moorhead, and A. Richter (2013), Carbon use efficiency of microbial communities: stoichiometry, methodology and modelling, *Ecology Letters*, n/a-n/a.

Six, J., S. D. Frey, R. K. Thiet, and K. M. Batten (2006), Bacterial and fungal contributions to carbon sequestration in agroecosystems, *Soil Science Society of America Journal*, *70*(2), 555-569.

Smits, N.A.C. & A.M. Kooijman (2012a), Herstelstrategie H2130A: Grijze duinen (kalkrijk). PAS-herstelstrategie.

Smits, N.A.C. & A.M. Kooijman (2012b), Herstelstrategie H2130A: Grijze duinen (kalkarm). PAS-herstelstrategie.

Strickland, M. S., and J. Rousk (2010), Considering fungal: Bacterial dominance in soils - Methods, controls, and ecosystem implications, *Soil Biology and Biochemistry*, *42*(9), 1385-1395.

van Genuchten, M. T. (1980), Closed-form equation for predicting the hydraulic conductivity of unsaturated soils, *Soil Science Society of America Journal*, *44*(5), 892-898.

Van der Hagen, H. (2011), Duingebied De Harstenhoek: ervaringen met Shetland pony's. De Levende Natuur 112(1):24-25.

Veer, M. A. C., and A. M. Kooijman (1997), Effects of grass-encroachment on vegetation and soil in Dutch dry dune grassland, *Plant and Soil*, *192*(1), 119-128.

Voortman, B. R., R. P. Bartholomeus, P. Van Bodegom, H. Gooren, E. A. T. M. van der Zee, and J. P. M. Witte (in prep.), Unsaturated hydraulic properties of xerophilous mosses: towards implementation of moss covered soils in hydrological models.

Walse, C., B. Berg, and H. Sverdrup (1998), Review and synthesis of experimental data on organic matter decomposition with respect to the effect of temperature, moisture, and acidity, *Environmental Reviews*, *6*(1), 25-40.

Wösten, J. H. M., G. J. Veerman, W. J. M. de Groot, and J. Stolte (2001), Waterretentie- en doorlatendheidskarakteristieken van boven- en ondergronden in Nederland: de Staringreeks, 86 pp, Alterra, Wageningen.

Appendix I. Estimates of C in $CaCO_3$

Estimate of C in $CaCO_3$

Our main analysis used soil total C measured by CN analyser. This include inorganic C, thus could lead to overestimation of soil organic C especially in lime-rich soils.

Although $CaCO_3$ content (%) was not explicitly measured, it can be roughly estimated as:

$$CaCO_3 = (soilC - 0.5 \cdot SOM) \cdot \frac{100.0869}{12.011}$$

where soilC is the soil total C (%) measured with CN analyzer (thus including C in CaCO3), SOM is the soil organic matter content (%) measured with loss on ignition (thus including organic C only), 100.0869 and 12.011 are the molecular weight of CaCO3 and C, respectively. For both soilC and SOM, we used the data of 2012 at soil depth of 0-5cm. CaCO2 was indeed much higher in the lime-rich sites (Figure 27).

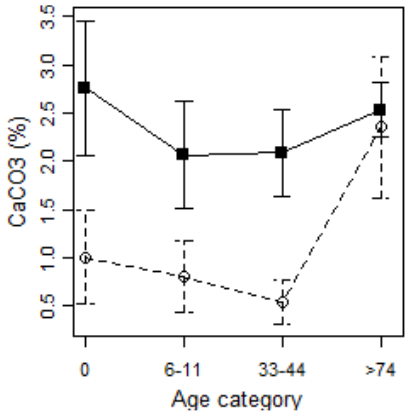

Figure 27. Mean values of CaCO3 (estimated in 2012 in the soil depth of 0-5cm) for each age category of lime-rich (filled squared) and lime-poor (open circles) sites. Bars indicate standard errors

Correction of overestimation of soil total C

Subsequently, the soil total C measured in 2013 in this study was corrected for the lime content as:

$$soilC\_cor = soilC - \frac{12.011}{100.0869} \cdot CaCO_3$$

where *soilC_cor* is the soil total C corrected for C in $CaCO_3$ (%). Furthermore, corrected values of soil N:C ratio (*soilNC_cor*), microbial C per soil total C (*MicC/C_cor*) and C mineralization rate per soil total C (*Cmin/C_cor*) were calculated.

Consequence of overestimation of soil total C on main findings

ANOVA tests with corrected values of *soilC*, *soilNC*, *MicC/C*, and *Cmin/C* showed that their patterns between lime class and between age categories remained unchanged (Figure 28, Tabel 3). This indicates that our main findings were not biased by the overestimation of soil total C.

Tabel 3. Results of 2-way ANOVA for soil variables which were correctd for C contained in $CaCO_3$. F values and their p-values are shown for the effect of lime category (lime-rich/lime-poor), age category (0/6-11/33-44/>74 years), and their interactions.

				ANOVA		
Description	**Unit**	**Abb.**	**N**	**Lime**	**Age**	**Interaction**
Soil total Carbon	%	*soilC_cor*	40	**11.177****	**93.276*****	0.363
Soil N:C ratio	gN/gC	*soilNC_cor*	40	1.168	**75.079*****	**2.906***
Microbial C per total soil C	gC/kgC	*MicC/C_cor*	23	**21.953*****	**7.962****	2.786
C mineralisation rate per soil total C	gC/gC/56d	*Cmin/C_cor*	40	1.445	**9.590*****	0.510

****: p<0.001, **: p<0.01, *: p<0.05, ns: not significant.*

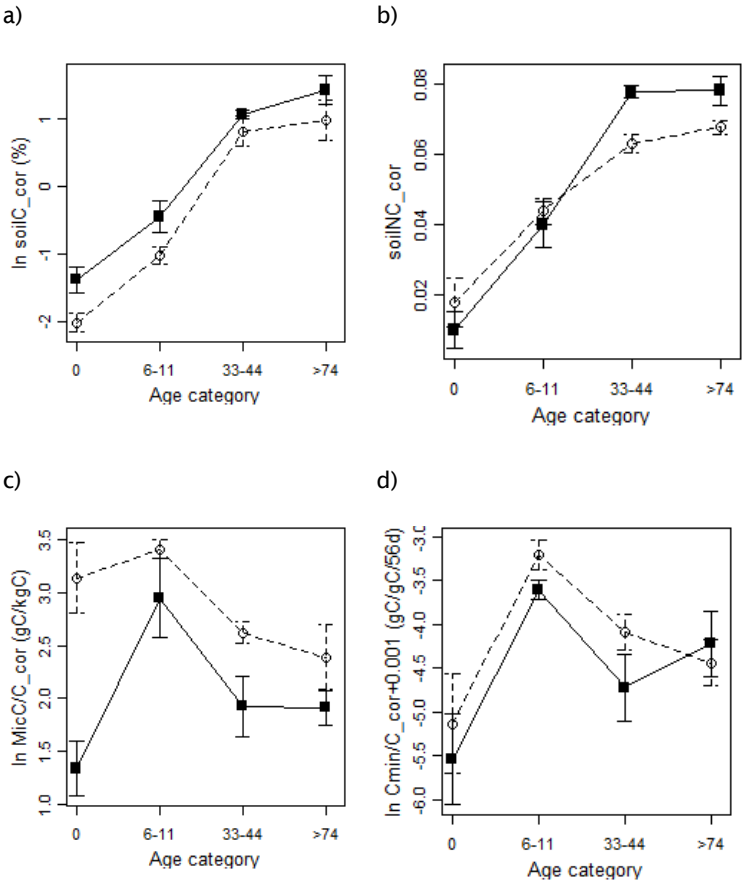

Figure 28. Mean values of a) soil total C, b) soil N:C ratio, c) microbial C per soil total C, and d) C mineralization rate per soil total C (all corrected for C in CaCO3) for each age category of lime-rich (filled squared) and lime-poor (open circles) sites. Bars indicate standard errors

Appendix II. Estimation of C mineralization in the soil during the incubation period

Respiration rates of incubated soils decrease in the course of time as soil substrates gradually deplete. To reflect that decrease in the estimates of cumulative C mineralization rates for the entire incubation period, C mineralisation rate was measured twice: once for all 50 samples at the beginning of incubation (*cmin1*, g C/ g d.w. soil/ h), and once for a subset of 30 samples at the end of incubation (*cmin2*, g C/ g d.w. soil/ h). *cmin1* was measured at the 5th day of the incubation, whereas *cmin2* was measured at the 55th day of incubation.

The subset of 30 samples which had data for both measurements were used to calculate the decrease in C mineralisation rate from the beginning to the end of the incubation. C mineralisation rates were square-root-transformed prior to calculation to correct for their right-skewed distribution. The decrease (in proportion) was estimated by fitting a linear regression model of *cmin2* regressed by *cmin1*. The regression line was forced through zero. Using the obtained regression model (R^2 = 0.949,Figure 29), we estimated *cmin2* of all 50 samples as follows:

$$cmin2 = 0.658 \cdot cmin1$$

With an assumption of linear decreases in C mineralization rates during the incubation period, the cumulative carbon mineralization over a period of 56 days (*Cmin*, g C/ g d.w. soil/ 56-day) was calculated using measured *cmin1* and estimated *cmin2* as:

$$Cmin = (cmin1+cmin2)/2 \cdot 24 \cdot 56$$

For the calculation of a sample (plot 16; age 0, lime poor), *Cmin* was calculated from measured *cmin2* and estimated *cmin1* (using the same regression coefficient), instead of measured *cmin1* and estimated *cmin2*, because *cmin1* was not properly measured.

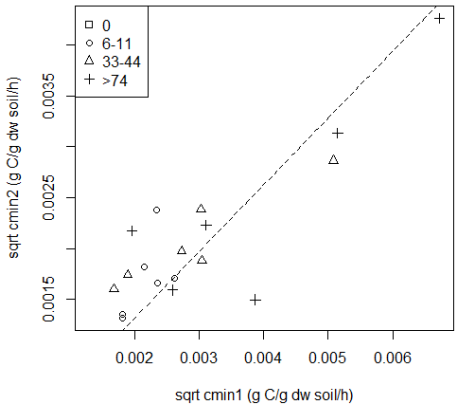

Figure 29. carbon mineralisation rate at day 5 against carbon mineralisation rate at day 55. The linear regression model is shown.

Appendix III. Structure and equations of CENTURY model

We built the CENTURY model with the programming language Python. The model consists of different processes (e.g. plant growth, plant death, SOM dynamics, nitrification and denitrification, hydrology, N leaching). We used the equations of CENTURY ver.4 [*Metherell et al.*, 1993] unless specified. The original CENTURY computes plant growth and death monthly, whereas we simulate them on a daily basis. Accordingly, some of the parameter values were adjusted (with a factor x1/30). All the other processes were computed on a daily basis too.

Plant growth

Potential growth

Potential maximum aboveground growth (gC / m^2 / day) is formulated as:

$$P_P = P_{\max} \cdot T_P \cdot M_P \cdot S_P$$

where P_{max} is the potential aboveground daily production (80 gC/m^2/day for temperate grasslands in CENTURY ver.4), T_P is the temperature effect on plant growth (-), M_P is the soil moisture effect on plant growth (-), S_P is the shading effect of dead materials on plant growth (-). For simplicity we assumed S_P to be 1.

T_P is formulated as:

$$T_P = \exp\left[\frac{1}{3.5}\cdot\left\{1-\left(\frac{32-SoilTemp}{32-15}\right)^{3.5}\right\}\right]\cdot\left(\frac{32-SoilTemp}{32-15}\right)$$

where *SoilTemp* is the soil temperature. Parameter values are for temperate grasslands ('TG' in CENTURY ver. 4).

M_P is formulated as:

$$M_P = \min\left(1, \max\left(0.01, 1-\frac{pptprd-0.8}{(afiel-awilt)-0.8}\cdot\right)\right)$$

$$pptprd = \frac{(ppt+h2o)}{pet}$$

where *afiel* and *awilt* is the water content of field capacity and wilting point of the top soil layer (fraction), *ppt* is the precipitation of the day (cm), *pet* is potential evapotranspiration of the day (cm), and *h2o* is the water stored at 0-60cm depth in previous day (cm).

Allocation of biomass to shoot and root is determined either as a function of time since planting or as a function of precipitation in CENTURY ver. 4. We calculated the fraction of allocation (f_R) to root using the latter option:

$$f_R = \frac{100 + 7 \cdot ppt}{60 + 14.7 \cdot ppt}$$

Using a typical annual precipitation of 80cm per year in the Netherlands, we set a constant f_R value of 0.534.

From this, the potential shoot growth (P_{PS}, gC/m^2/day) and root growth (P_{PR}, gC/m^2/day) are expressed as:

$$P_{PS} = P_P$$
$$P_{PR} = \frac{f_R}{1 - f_R} \cdot P_P$$

Total (i.e. below + aboveground) potential production (P_{PT}, gC/m^2/day) is:

$$P_{PT} = P_{PS} + P_{PR}$$

Actual growth

Actual plant growth (P_A, gC/m^2/day) is determined by the availability of essential nutrients. Here we only consider Nitrogen. Suppose that C:N ratio of shoot can deviate between maximum ($CN\max_S$) and minimum ($CN\min_S$) values, and C:N ratio of root between maximum ($CN\max_R$) and minimum ($CN\min_R$) values. $CN\max_R$ and $CN\min_R$ was set as constant values, 55 and 50 (CENTURY ver. 4). $CN\max_S$ and $CN\min_S$ were calculated as a function of biomass as:

$$CN\max_S = \min\left(95, 35 + 0.15 \cdot Biomass\right)$$
$$CN\min_S = \min\left(90, 30 + 0.15 \cdot Biomass\right)$$

where *Biomass* is above-ground plant biomass (gC biomass/m^2). Parameter values are for C3 grasses ('G1' in CENTURY ver. 4).

The minimum and maximum CN ratios of the whole biomass ($CN\max_W$ and $CN\min_W$) can be calculated as:

$$CNmin_W = \frac{1}{f_R / CNmin_R + (1 - f_R) / CNmin_S}$$
$$CNmax_W = \frac{1}{f_R / CNmax_R + (1 - f_R) / CNmax_S}$$

When N availability (Nava) is lower than what is needed to realize the maximum CN ratio, actual plant production is reduced:

$$P_A = \begin{cases} P_{PT} & Nava \geq \dfrac{P_{PT}}{CNmin_{\mathrm{W}}} \\ P_{PT} & \dfrac{P_{PT}}{CNmin_{\mathrm{W}}} > Nava \geq \dfrac{P_{PT}}{CNmax_{\mathrm{W}}} \\ Nava \cdot CNmax_{\mathrm{W}} & \dfrac{P_{PT}}{CNmax_{\mathrm{W}}} > Nava \end{cases}$$

Amount of N in shoot (N_S) and roots (N_R) (gN / m^2) in the newly-produced biomass are calculated as:

$$N_S = \begin{cases} \dfrac{P_A \cdot (1 - f_R)}{CNmin_{\mathrm{S}}} & Nava \geq \dfrac{P_{PT}}{CNmin_{\mathrm{W}}} \\ Nava \cdot \dfrac{(1 - f_R) \cdot CNmin_{\mathrm{S}}}{f_R \cdot CNmin_{\mathrm{R}} + (1 - f_R) \cdot CNmin_{\mathrm{S}}} & \dfrac{P_{PT}}{CNmin_{\mathrm{W}}} > Nava \geq \dfrac{P_{PT}}{CNmax_{\mathrm{W}}} \\ \dfrac{P_A \cdot (1 - f_R)}{CNmax_{\mathrm{S}}} & \dfrac{P_{PT}}{CNmax_{\mathrm{W}}} > Nava \end{cases}$$

$$N_R = \begin{cases} \dfrac{P_A \cdot f_R}{CNmin_{\mathrm{R}}} & Nava \geq \dfrac{P_{PT}}{CNmin_{\mathrm{W}}} \\ Nava \cdot \dfrac{f_R \cdot CNmin}{f_R \cdot CNmin_{\mathrm{R}} + (1 - f_R) \cdot CNmin_{\mathrm{S}}} & \dfrac{P_{PT}}{CNmin_{\mathrm{W}}} > Nava \geq \dfrac{P_{PT}}{CNmax_{\mathrm{W}}} \\ \dfrac{P_A \cdot f_R}{CNmax_{\mathrm{R}}} & \dfrac{P_{PT}}{CNmax_{\mathrm{W}}} > Nava \end{cases}$$

Mineral form of N in soil is available for plant uptake, and is restricted by root biomass: with a factor *rtimp* (fraction):

$$Nava = mineralN \cdot rtimp$$

$$rtimp = 1 - 0.8 \cdot \exp(-0.015 \cdot rootC \cdot 2.5)$$

where *mineralN* is mineral N in soil(gN/m2), *rtimp* is the reduction factor of root biomass on N availability (fraction, 0-1), *rootC* is the amount of C in root (gC/m2).

Lignin content

Lignin content (fraction of C) in shoot (L_S) and root (L_R) are calculated as:

$$L_S = 0.0012 \cdot ppt + 0.02$$

$$L_R = -0.0015 \cdot ppt + 0.26$$

where *ppt* is the annual precipitation (cm). Using a typical annual precipitation of 80cm per year in the Netherlands, we set a constant L_S value of 0.116 and L_R value of 0.14.

Plant Death

Shoots die every day in growing season with a rate depending on soil moisture:

$$d_S = fsdeth \cdot \left(1 - \frac{1}{1 + 4 \cdot \exp(-6 \cdot rwcf)}\right)$$

$$rwcf = \frac{swater - awilt}{afiel - awilt}$$

where d_s is the death rate of shoot (day^{-1}), *fsdeth* is the maximum death rate (0.2/30 day^{-1}), *rwcf* is relative soil water content, *swater* is the daily average soil water in the top soil layer (cm3/cm3). CENTURY ver.4 also includes shoot death due to shading, which was omitted in this study.

On the first day of the senescence month, shoots die with a constant rate of 0.95 (day^{-1}).

Roots die, when soil temperature is higher than 2ºC, with a rate depending on soil moisture:

$$d_R = rdr \cdot \left(1 - \frac{1}{1 + 4 \cdot \exp(-6 \cdot rwcf)}\right)$$

where d_R is the death rate of shoot (day^{-1}), *rdr* is the maximum death rate (0.05/30 day^{-1}).

CENTURY ver. 4 can include additional shoot death due to shading, which is not included here.

Transformation of dead plant materials

Dead shoots become standing dead materials. The standing dead materials are transformed into surface litters with a constant rate of 0.15/30 (day^{-1}). The division into metabolic and structural surface litter is a function of lignin to N ratio in the litter:

$$frmet = 0.99 - 0.018 \cdot L_S / N_S$$

$$frstr = 0.01 + 0.018 \cdot L_S / N_S$$

where *frmet* is the fraction of standing dead materials going to metabolic surface litter (-), *frstr* is the fraction of standing dead materials going to structural surface litter (-).

The same fractions (*frmet* and *frstr*) are used to divide dead roots into metabolic and structural root litter.

SOM dynamics

C flows

Carbon flows of litter and soil organic pools are formulated according to CENTURY ver. 4:

$$\frac{dC_i}{dt} = -k_i \cdot C_i + \sum_j f_{ji} \cdot k_j \cdot C_j$$

$$\mathbf{K} = \begin{pmatrix} k_1 \\ k_2 \\ k_3 \\ k_4 \\ k_5 \\ k_6 \\ k_7 \\ k_8 \\ k_9 \end{pmatrix} = Md \cdot Td \cdot Pd \cdot \begin{pmatrix} kmax_1 \cdot e^{(-3 \cdot L)} \\ kmax_2 \\ kmax_3 \cdot e^{(-3 \cdot L)} \\ kmax_4 \\ kmax_5 \\ kmax_6 \cdot (1 - 0.75 \cdot Tex) \\ kmax_7 \\ kmax_8 \\ 0 \end{pmatrix}$$

$$\mathbf{F} = \begin{pmatrix} f_{11} & \cdots & f_{19} \\ \vdots & \ddots & \vdots \\ f_{91} & \cdots & f_{99} \end{pmatrix} = \begin{pmatrix} 0 & 0 & 0 & 0 & f_{15} & 0 & f_{17} & 0 & f_{19} \\ 0 & 0 & 0 & 0 & f_{25} & 0 & 0 & 0 & f_{29} \\ 0 & 0 & 0 & 0 & 0 & f_{36} & f_{37} & 0 & f_{39} \\ 0 & 0 & 0 & 0 & 0 & f_{46} & 0 & 0 & f_{49} \\ 0 & 0 & 0 & 0 & 0 & 0 & f_{57} & 0 & f_{59} \\ 0 & 0 & 0 & 0 & 0 & 0 & f_{67} & f_{68} & f_{69} \\ 0 & 0 & 0 & 0 & 0 & f_{76} & 0 & f_{78} & f_{79} \\ 0 & 0 & 0 & 0 & 0 & f_{86} & 0 & 0 & f_{89} \\ 0 & 0 & 0 & 0 & 0 & 0 & 0 & 0 & 0 \end{pmatrix}$$

$$f_{15} = (1 - L_S) \cdot 0.4$$
$$f_{17} = L_S \cdot 0.7$$
$$f_{19} = (1 - L_S) \cdot 0.6 + L_S \cdot 0.3$$
$$f_{25} = 0.4$$
$$f_{29} = 0.6$$
$$f_{36} = (1 - L_R) \cdot 0.45$$
$$f_{37} = L_R \cdot 0.7$$
$$f_{39} = (1 - L_R) \cdot 0.55 + L_R \cdot 0.3$$
$$f_{46} = 0.45$$
$$f_{49} = 0.55$$
$$f_{57} = 0.4$$
$$f_{59} = 0.6$$
$$f_{67} = 1 - 0.85 + 0.68 \cdot Tex - 0.003 - 0.032 \cdot Tex$$
$$f_{68} = 0.003 + 0.032 \cdot Tex$$
$$f_{69} = 0.85 - 0.68 \cdot Tex$$
$$f_{76} = 0.45 - 0.003 - 0.009 \cdot Clay$$
$$f_{78} = 0.003 + 0.009 \cdot Clay$$
$$f_{79} = 0.55$$
$$f_{86} = 0.45$$
$$f_{89} = 0.55$$

where *Ci* is the carbon content of pool *i* (gC m^{-2} day^{-1}), *Md* is the reduction factor on decomposition due to soil moisture (fraction), *Td* is the reduction factor on decomposition due to soil temperature (fraction), *Pd* is the reduction factor on decomposition due to pH (fraction), L_S and L_R are the lignin content (fraction in relation to C content) of plant shoots and roots respectively, *Tex* is the fraction of clay and silt, *Clay* is the fraction of clay. Maximum decomposition rates of different pools are: $kmax_1$=3.9 ($year^{-1}$), $kmax_2$=14.8 ($year^{-1}$),

$kmax_3$=4.9 (year^{-1}), $kmax_4$=18.5 (year^{-1}), $kmax_5$=6.0 (year^{-1}), $kmax_6$=7.3 (year^{-1}), $kmax_7$=0.2 (year^{-1}), $kmax_8$=0.0066 (year^{-1}).

The temperature reduction term, *Td*, was defined according to CENTURY ver. 4 [*Metherell et al*., 1993]:

$$Td = 0.08 \cdot \exp\left(0.095 \cdot Temp\right)$$

where *Temp* is the mean of daily maximum and minimum air temperature (degrees Celsius).

The moisture reduction term, *Md*, was defined according to *Fujita et al*. [2013]:

$$Md = f_{\mathrm{d}} \cdot f_{\mathrm{w}}$$

$$f_{\mathrm{d}} = \begin{cases} 1 & \psi_{\mathrm{B}} \le \psi \\ 1 - \dfrac{\log(|\psi|) - \log(|\psi_{\mathrm{B}}|)}{\log(|\psi_{\mathrm{A}}|) - \log(|\psi_{\mathrm{B}}|)} & \psi_{\mathrm{A}} \le \psi < \psi_{\mathrm{B}} \\ 0 & \psi < \psi_{\mathrm{A}} \end{cases}$$

$$f_{\mathrm{w}} = \begin{cases} 1 & \varphi_{gas\_th} \le \varphi_{gas} \\ \dfrac{\varphi_{gas}}{\varphi_{gas\_th}} \cdot (1-m) + m & \varphi_{gas} < \varphi_{gas\_th} \end{cases}$$

where f_{d} is the reduction term in dry condition (fraction), f_{w} is the reduction term in wet conditions (fraction), ψ is the matric potential in top soil (kPa), ψ_{A} and ψ_{B} are the threshold values of matric potential (ψ_{A} = -13800 kPa and ψ_{B} = -29 kPa), φ_{gas} is the gas content in top soil (cm^3/cm^3), φ_{gas_th} is the threshold of gas content where oxygen stress start (φ_{gas_th} =0.2 cm^3/cm^3), and *m* is the level of anaerobic decomposition as a proportion to that of aerobic decomposition (*m*=0.24).

The pH reduction term, *Pd*, was defined in the main text.

N flows

N flows were coupled with C flows. The outflow of N is proportional to that of C, whereas the inflow of N into a pool is the product of the C inflow into the pool and the optimum N:C ratio of the pool (nc_i). The N flows from pool *i* (gN m^{-2} day^{-1}) are formulated as:

$$\frac{dN_i}{dt} = -k_i \cdot N_i + \sum_j f_{ji} \cdot k_j \cdot C_j \cdot nc_j$$

Although later versions of CENTURY (after version 3.0) allow flexible N:C ratios in metabolic litter pools and SOM pools depending on N content of incoming plant residues and mineral N content respectively, we used fixed N:C ratios as in the original CENTURY for simplicity.

N is mineralized if in excess, and immobilized from mineral N pool if in shortage. The amount of mineralized N associated with the flows to pool *i* , μ_i, (gN m^{-2} day^{-1}) is expressed as:

$$\mu_i = \sum_j f_{ji} \cdot k_j \cdot C_j \cdot \left(\frac{N_j}{C_j} - nc_i\right)$$

Note that μ_i represent net N mineralization when positive and net N immobilization when negative.

The total N mineralization rate M (gN m^{-2} day^{-1}) is calculated as:

$$M = \sum_i \mu_i$$

Reduction on decomposition due to climatic conditions (*Td, Md*)

Temperature reduction term on decomposition, *Td*, was formulated according to CENTURY ver. 4:

$$Td = 0.08 \cdot \exp(0.095 \cdot temp)$$

where *temp* is the soil temperature (˚C).

Soil moisture reduction term on decomposition, *Md*, was taken from *Fujita et al.* [2013], which was validated for a wide range of Dutch natural ecosystems:

$$Md = f_d \cdot f_w$$

$$f_d = \begin{cases} 1 & \psi_B \le \psi \\ 1 - \dfrac{\log(|\psi|) - \log(|\psi_B|)}{\log(|\psi_A|) - \log(|\psi_B|)} & \psi_A \le \psi < \psi_B \\ 0 & \psi < \psi_A \end{cases}$$

$$\psi = 0.0981 \cdot \frac{1}{\alpha} \cdot \left[\left(\frac{\theta_{sat} - \theta_{res}}{\theta - \theta_{res}} \right)^{\frac{n}{n-1}} - 1 \right]^{\frac{1}{n}}$$

$$f_w = \begin{cases} 1 & \varphi_{gas\_th} \le \varphi_{gas} \\ \dfrac{\varphi_{gas}}{\varphi_{gas\_th}} \cdot (1-m) + m & \varphi_{gas} < \varphi_{gas\_th} \end{cases}$$

where f_d and f_w are negative effects of dry conditions and wet conditions respectively, ψ is the matric potential (kPa), ψ_A and ψ_B are threshold values of matric potential (ψ_A=-13.8MPa, ψ_B= -0.029 MPa), φ_{gas} is the soil gas content (cm^3 cm^{-3}), θ_{res} and θ_{sat} are the residual and saturated soil water content respectively (cm^3 cm^{-3}), α and n are the scaling parameters, φ_{gas_th} is the threshold of soil gas content where oxygen stress starts (φ_{gas_th} =0.2 (cm^3 cm^{-3})), and m is the level of anaerobic decomposition as a proportion to that of aerobic decomposition when soil is saturated (m=0.24 (-)). θ_{res}, θ_{sat}, α, and n are site-specific soil physical parameters.

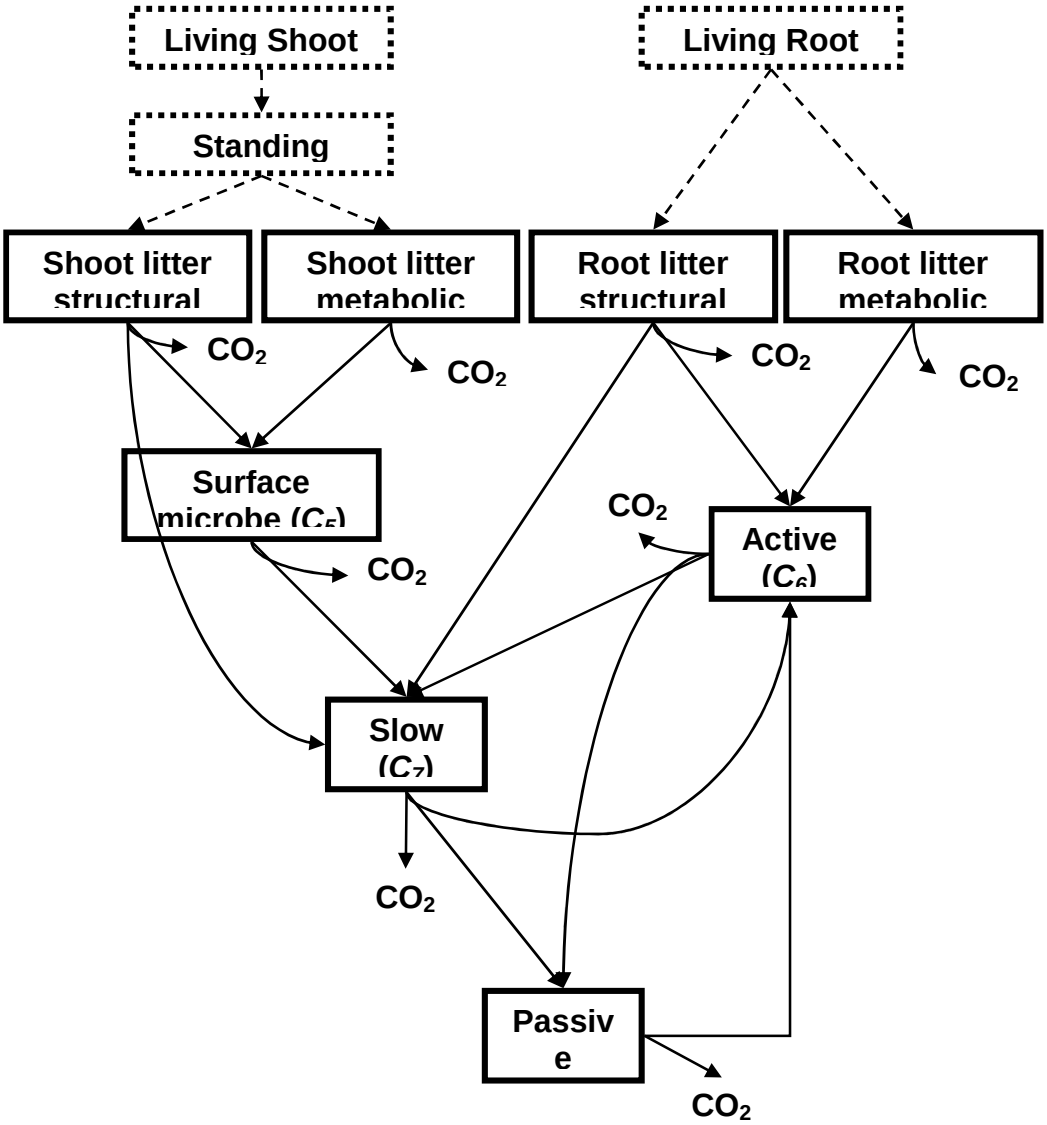

Figure. Structure of litter and SOM dynamics of CENTURY. Solid arrows represent C flow rates. State variables in dotted box and dotted arrows represent the pools and flows of plant biomass, which were defined in the previous section.

Nitrification and Denitrification

Nitrification

We used the equations of the daily version of CENTURY, DAYCENT [*Del Grosso et al.*, 2002], to simulate nitrification processes. The rate of NH_4 oxidation is described by a first-order kinetics as:

$$Nit = k_{nit} \cdot [N - NH_4] \cdot fNw$$

where *Nit* is the nitrification rate (mg N kg soil^{-1} day^{-1}), k_{nit} is the maximum nitrification rate (day^{-1}), [N-NH_4] is the concentration of N-NH_4 in soil (mg N kg soil^{-1}), and *fNw* is the reduction term of soil moisture (-). k_{nit} is set to be 0.15 day^{-1}.

Nitrification rate increases with increasing water content in soil pore space, reaching the maximum at field capacity, and then reduces to zero when the soil pore space is filled with water:

$$fNw = \begin{cases} \left(1 + 30 \cdot \exp(-9 \cdot \frac{\theta - \theta_{wp}}{\theta_{fc} - \theta_{wp}})\right)^{-1} & \theta \le \theta_{fc} \\ \frac{\theta_{sat} - \theta}{\theta_{sat} - \theta_{fc}} & \theta_{fc} < \theta \end{cases}$$

where θ is the volumetric water content in soil (cm^3 cm^{-3}), θ_{wp}, θ_{fc} and θ_{sat} are the soil water contents at wilting point, field capacity, and saturation (cm^3 cm^{-3}), respectively. This formulation is similar to other nitrification models [e.g. *Porporato et al.*, 2003].

The pH effect was omitted here because none of our plots had the very low pH where strong inhibition effect occurs (pH lower than 3).

Denitrification

According to DAYCENT ([*Del Grosso et al.*, 2002], denitrification rate was formulated as a function of N-NO_3 concentration, CO_2 concentration (as a proxy for labile C), and soil moisture conditions:

$$Denit = MIN(fDno_3, fDco_2) \cdot fDw$$

where *Denit* is the denitrification rate (mg N kg soil^{-1} day^{-1}), $fDno_3$ is the denitrification rate limited by NO_3 concentration (mg N kg soil^{-1} day^{-1}), $fDco_2$ is the denitrification rate limited by CO_2 concentration (mg N kg soil^{-1} day^{-1}), and *fDw* is the reduction factor due to soil moisture (-).

The effects of NO_3 and CO_2 on denitrification rate were formulated based on the empirical relationships obtained by an incubation experiment [*Del Grosso et al.*, 2000]:

$$fDno3 = MIN(0, 1.556 + \frac{76.91}{\pi} \cdot \arctan\{\pi \cdot 0.00222 \cdot ([N - NO_3] - 9.23)\})$$

$$fDco_2 = 0.1 \cdot [CO_2]^{1.3}$$

where [N-NO_3] is the concentration of nitrate in soil (mgN kg soil^{-1}), [CO_2] is the respired C during the day (mg C kg soil^{-1}).

As soil moisture increases, the air-filled pore space decreases (i.e. the preferential e^- acceptor O_2 decreases) and therefore denitrification rate increases. The threshold value of soil moisture depends on soil texture as well as oxygen demand in the soil [*Del Grosso et al.*, 2000]. The latter is related to the amount of e^- donor, labile C, which can be approximated by amount of respiration. Soils with low gas diffusivity, such as clay, are prone to the effect of O_2 demand because O_2 diffuses slowly and therefore microsite anoxia emerges more often. The reduction term of soil moisture is denoted as:

$$fDw = 0.45 + \frac{\arctan(6 \cdot \pi \cdot (\theta / \theta_{sat} - x)}{\pi}$$

$$x = 0.9 - 0.1 \cdot M \cdot MIN([CO_2], 20)$$

$$M = -1.25 \cdot MIN(0.113, dfc) + 0.145$$

where x is the inflection point of soil moisture where denitrification rate increases rapidly (in the unit of water filled pore space (-)), M is the multiplier which determines the strength of the CO_2 effect on the inflection point, *dfc* is the gas diffusivity coefficient at field capacity. We set a maximum value for the CO_2 effect on the inflection point ($[CO_2]$ = 20 mg C kg soil^{-1}) below which CO_2 is not the dominant limiting factor for denitrification [*Del Grosso et al*., 2000].

The gas diffusivity coefficient at field capacity is a soil specific value, and was calculated according to *Moldrup et al*. [2000]:

$$dfc = 2 \cdot \left(\frac{\theta_{sat} - \theta_{fc}}{\theta_{sat}} \right)^3 + 0.04 \cdot \left(\frac{\theta_{sat} - \theta_{fc}}{\theta_{sat}} \right)$$

Hydrological model (Bucket model)

A simple bucket model of CENTURY model [*Parton et al.*, 1993] was used. Snow and liquid snow were omitted. Soil was separated into three soil layers, for each of which soil physical parameters were derived from 1:50,000 soil maps. Plant-related parameters (living biomass, standing dead materials, surface litter) were updated every month from the plant module of the model. See Table for specifications of the variables.

$$\frac{dS_1}{dt} = ADD - EVBS - F_1 - T_1$$

$$ADD = ppt - EVAP$$

$$EVAP = \min\{(INT + BS)\cdot ppt,\ pet\}$$

$$INT = (0.3\cdot ld + 0.6\cdot sd)\cdot 0.0008$$

$$BS = 0.4\cdot \exp\{-0.01\cdot(0.2\cdot ld + 0.4\cdot sd)\}$$

$$EVBS = \max\{0,\ 0.33\cdot EV\cdot BS\cdot(pet - EVAP - TR)\}$$

$$EV = \max\left(0,\ \frac{RWC_1 - 0.25}{1 - 0.25}\right)$$

$$RWC_1 = \frac{S_{1,t-1} - swp_1}{sfc_1 - swp_1}$$

$$TR = \min(FAV,\ Tp)$$

$$FAV = \max\left(0,\ \sum_{i=1}^{3}(S_{1,t-1} - swp_1)\right)$$

$$Tp = \min[pet - EVAP,\ 0.65\cdot\{1 - \exp(-0.02\cdot lb)\}]$$

$$F_1 = \max(0,\ S_{1,t-1} - sfc_1)$$

$$T_i = \min\left(S_{i,t-1},\ TR\cdot\frac{W_i}{Ws}\right) \qquad for\ i = \{1,2,3\}$$

$$W_i = FWC_i\cdot awl_i\cdot a_i$$

$$FWC_i = \max(0,\ S_{i,t-1} - swp_i)$$

$$Ws = \sum_{i=1}^{3} W_i$$

$$\frac{dS_2}{dt} = F_1 - F_2 - T_2$$

$$F_2 = \max(0,\ S_{2,t-1} - sfc_2)$$

$$\frac{dS_3}{dt} = F_2 - F_3 - T_3 - SF$$

$$F_3 = \max\{0,\ (1 - kf)\cdot(S_{3,t-1} - sfc_3)\}$$

$$SF = \max\{0,\ kf\cdot(S_{3,t-1} - sfc_3)\}$$

$$\frac{dD}{dt} = F_3 - SS$$

$$SS = kx\cdot D_{t-1}$$

Variable	Unit	Value	Description
$S_{i,t}$	cm		Soil water in layer i at day i
D_t	cm		deep H2O storage at day t
dS_i/dt	cm/day		Rate of change of S_i
dD/dt	cm/day		Rate of change of D
ADD	cm/day		water added to the soil
EVAP	cm/day		bare soil plus interception H2O loss
INT	fraction		fraction of PPT lost as interception H2O loss
BS	fraction		fraction of PPT lost as bare soil H2O loss
EVBS	cm/day		bare soil evapotranspiration
EV	fraction		fraction of water content between 'fwlos' and field capacity ('fwlos' = 0.25; minimum relative water content for top layer to evaporate)
RWC_i	fraction		relative water content of layer i
TR	cm/day		total transpiration H2O loss
FAV	cm/day		total H2O available for transpiration H2O loss
Tp	cm/day		potential transpiration H2O loss
F_i	cm/day		saturated H2O flow from layer 1 to 2 (i=1), 2to 3 (i=2), and 3 to deep strage (i=3)
T_i	cm/day		transpiration H2O loss from layer i
W_i	fraction		weight factor for transpiration H2O loss from layer i
Ws	fraction		sum of W_i
SF	cm/day		stream flow
SS	cm/day		H2O flow from deep strage to stream
ppt	cm/day	s.s.	daily precipitation
pet	cm/day	s.s.	daily evapotranspiration
ld	g/m^2	200	surface litter biomas
sd	g/m^2	400	standing dead + live biomass

lb	g/m^2	300	aboveground live plant biomass
swp_i	cm	s.s.	Water content at wilting point for layer i
sfc_i	cm	s.s.	Water content at field capacity for layer i
awl_i	fraction	s.s.	relative root density in layer i
a_i	cm	s.s.	depth of soil layer i
kf	fraction	0.6	fraction of flow from the bottom layer which goes into stream
kx	fraction	0.3	fraction of the soil water in deep storage which goes into stream

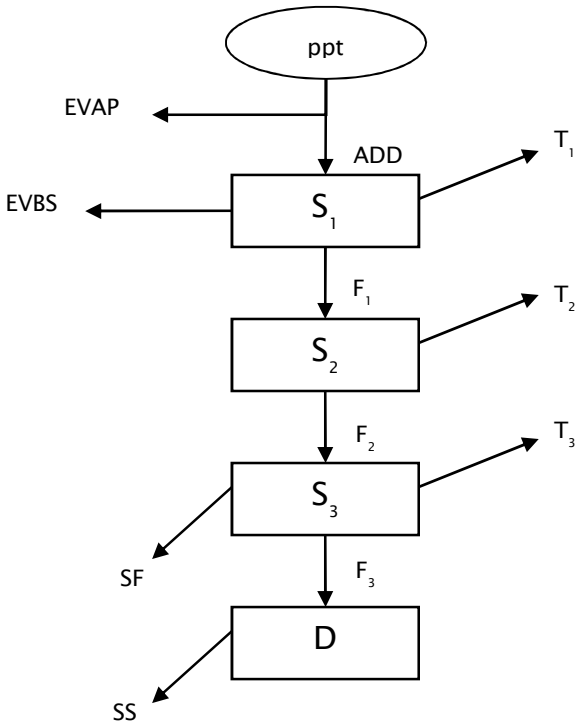

Figure. Structure of Hydrological model of CENTURY.

N leaching

Transfer of dissolved nitrogen (N-NH4 + N-NO3) in soil was calculated as the products of the water flows and the concentration of dissolved N in the originating layer. Daily N leaching rate was calculated as the sum of N transfer from S3 layer into stream and from D layer into stream ($gN/m^2/day$). N leaching is simulate daily after plant uptake of nitrogen.

Appendix IV. Restoration measures and its effects on nutrient status, base status and restoration of grey dune vegetation

The listed effects in the table include results of this study, the study of Aggenbach et al. (2013) and general knowledge. The measures are the same as listed in the restoration strategy of Smits & Kooijman (2012). The measures with in yellow are supposed potentially highly effective. Items in orange include a SOM and N accumulation effect of a high N-deposition in the past. Items in red are influenced by current and future N-deposition level.

measure	direct effect	effect on nutrient status	effect on base status	effect on restoration of grey dunes	
				response time after measure	sustainability when restored
topsoil excavation	- removes vegetation and complete humus profile	- strong decline of N and P pool, removal of accumulated N by deposition -> strong decline of N-mineralisation	- depending on soil base profile and excavation depth	- after 2-3 decades	depending on current and future N-deposition and soil base profile
sod cutting	- removes vegetation and all or greater part of humus profile	- strong decline of N and P pool, removal of accumulated N by deposition -> strong decline of N-mineralisation, depending on sod cut depth	- depending on soil base profile and sod cut depth	- when humus profile completely removed: restoration after 2-3 decades; - when humus profile partly removed and at small scale: faster restoration?	depending on current and future N-deposition and soil base profile
chopper	- removes vegetation and litter horizon	less strong decline of N and P pool, removal of accumulated N by deposition -> decline of N-mineralisation, quantitative effect unknown - N-mineralisation strongly depends on accumulated SOM -> effect of N-deposition on SOM accumulation	- possibly removal of relatively acid litter layer, removal of base cations -> decline of acid buffer capacity	- few years? - depending on soil N-mineralisation? and base status	?
mowing and removal of hay	- removes aboveground herb and grass vegetation	- some removal of N and P pool -> weak or no effect on N mineralisation? quantitative effect unknown, effect depends on frequency - N-mineralisation strongly depends on accumulated SOM -> effect of N-deposition on SOM accumulation	- removal of base cations -> decline of acid buffer capacity, effect depends on frequency	- few years? -depending on soil N-mineralisation? and base status	?

measure	direct effect	effect on nutrient status	effect on base status	effect on restoration of grey dunes	
				response time after measure	sustainability when restored
grazing by cattle, sheep	- removes aboveground herb and grass vegetation, may stimulate aeolian activity, trampling of dune soils	- faster turnover of nutrients? effect on soil nutrient status ? - N-mineralisation strongly depends on accumulated SOM -> effect of N-deposition on SOM accumulation	- faster turnover of base cations	- variable?, - depending on soil N-mineralisation? and base status	depending on current and future N-deposition and soil base profile
removal of	- removes shrubs	depends of combination with other measures			
burning	-changes aboveground herb and grass vegetation, litter horizon into ashes	- removal of N stock in above ground vegetation+litter - fast transfer of P and K in vegetation+litter to soil mineral P and K	- change of basic cation pool in above ground vegetation +litter to base cation pool in soil -> increase of soil base saturation? -> increase of pH depending soil base status	- few years?	depending on current and future N-deposition and soil base profile
restoring aeolian dynamics	-development of white dunes, secondary blowouts sedimentation of sand	- blowouts: removal most of N and mayor part of P pool -> new habitat with low N-mineralisation zones with aeolian sedimentation: - deposition of N poor sand, effects depends on sedimentation intensity - sand deposition in grasslands with humus profile may change N-mineralisation by change in pH and soil moisture conditions - what happens with the N and P removed from blowouts?	- depends on soil base profile and type of aeolian activity in superficial decalcificated dune areas increase locally increase of base status	- blowouts: after stabilisation 2-3 decades - zones with strong aeolian sedimentation: after stabilisation 2-3 decades - zones with weak aeolian sedimentation: faster?, time scale unknown, when deposited sand is lime rich/ base rich possibly positive	depending on current and future N-deposition and soil base profile